ACCELERATION OF THE SOLAR WIND†

EGIL LEER*, THOMAS E. HOLZER, and TOR FLÅ*

*High Altitude Observatory, National Center for Atmospheric Research**, Boulder, CO 80307, U.S.A.*

Abstract. In this review, we discuss critically recent research on the acceleration of the solar wind, giving emphasis to high-speed solar wind streams emanating from solar coronal holes. We first explain why thermally driven wind models constrained by solar and interplanetary observations encounter substantial difficulties in explaining high speed streams. Then, through a general discussion of energy addition to the solar wind above the coronal base, we indicate a possible resolution of these difficulties. Finally, we consider the question of what role MHD waves might play in transporting energy through the solar atmosphere and depositing it in the solar wind, and we conclude by examining, in a simple way, the specific mechanism of solar wind acceleration by Alfvén waves and the related problem of accelerating massive stellar winds with Alfvén waves.

1. Introduction

On the basis of observations of continuous auroral activity (Birkeland, 1908, 1913), 27-day recurrent geomagnetic activity (e.g., Chapman and Bartels, 1940), and the anti-solar alignment of ionized comet tails (Biermann, 1951), it has long been suspected that the Sun emits ionized particles continuously. In 1958, Parker suggested a physical mechanism whereby the predominantly hydrogen plasma of the Sun's outer atmosphere could be accelerated to supersonic speeds and thus flow continuously away from the Sun, through interplanetary space, as the solar wind. Parker (1958) argued that, given the high temperature (and the consequent high thermal conductivity (Chapman, 1957)) of the solar corona and the low pressure of the interstellar medium, the only possible steady state of the outer solar atmosphere is a supersonic expansion driven by the thermal pressure gradient force. The existence of the solar wind was subsequently confirmed by *in situ* spacecraft observations outside the terrestrial magnetosphere (Gringauz *et al.*, 1960, 1961, 1967; Bonetti *et al.*, 1963; Scherb, 1964; Snyder and Neugebauer, 1964). These and later observations (e.g., reviews by Axford, 1968; Hundhausen, 1972; Feldman *et al.*, 1977) indicated a high degree of variability of most solar wind parameters in lower-speed wind and a relative uniformity of most parameters in high-speed wind (so-called high-speed streams). The high-speed solar wind streams (Neugebauer and Snyder, 1966) were found frequently to recur with approximately a 27-day period (the solar rotation period as viewed from the Earth), and these recurrent streams were associated with the 27-day recurrent geomagnetic activity. By implication, the solar sources of high-speed streams were taken to be the, as yet unidentified, solar M-regions, which had been invoked as the solar sources of recurrent geomagnetic activity (e.g., Chapman and Bartels, 1940). Solar and interplanetary observations during and after the 1973-4 Skylab period led to the identification of these M-regions as solar

† Paper presented at the IX-th Lindau Workshop 'The Source Region of the Solar Wind'.

* On leave from the Auroral Observatory, Institute of Mathematical and Physical Sciences, University of Tromsø, N-9001 Tromsø, Norway.

** The National Center for Atmospheric Research is sponsored by the National Science Foundation.

Space Science Reviews **33** (1982) 161–200. 0038–6308/82/0332–0161$06.00.

coronal holes (Krieger *et al.*, 1973; Neupert and Pizzo, 1974; Bell and Noci, 1976; Hansen *et al.*, 1976; Hundhausen *et al.*, 1978; Nolte *et al.*, 1976; Sheeley *et al.*, 1976; Wagner, 1976; Hundhausen, 1977). The relationship among coronal holes, high-speed streams, and geomagnetic activity is illustrated in Figure 1.

It was realized by Parker (1965) that, while a purely thermally driven wind could readily produce the observed low to moderate solar wind speeds, the high-speed wind might require the addition of energy to the wind above the coronal base. In fact, it is

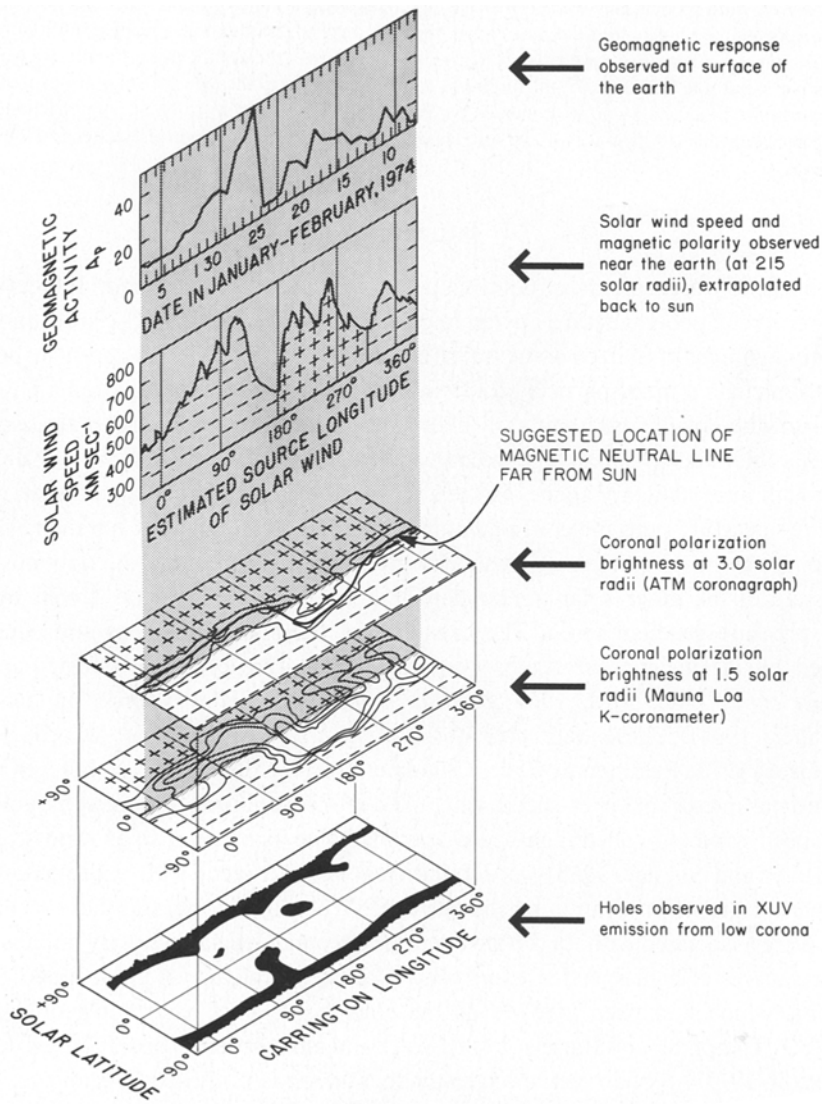

Fig. 1. The three-dimensional relations among coronal hole observations at different heights in the solar atmosphere, the solar wind structure observed in the ecliptic plane, and the resulting geomagnetic activity for Carrington solar rotation 1610, in early 1974. The magnetic polarity is indicated by + signs for magnetic fields pointing out of the Sun and − signs for fields pointing into the Sun (from Hundhausen and Holzer, 1980).

readily shown that if the solar wind temperature monotonically decreases from the coronal base to the orbit of Earth, the observational constraints of modest solar wind mass-flux densities in high-speed streams and moderate plasma pressures at the base of coronal holes require such extended energy addition in the region of supersonic flow (Holzer and Leer, 1980; Leer and Holzer, 1980). Hence, observations of high-speed streams and coronal holes place the most stringent requirements on theoretical descriptions of solar wind acceleration; these requirements are the most complete, as well, because of the unambiguous identification of coronal holes as the solar source of high speed streams and the extensive observations of coronal holes currently available. It seems appropriate, therefore, that in the present review of solar wind acceleration we concentrate primarily on coronal holes and high-speed solar wind streams.

We shall begin by considering models of thermally driven winds with no energy added above the coronal base (Section 2) and then discuss the general effects of energy addition (in the forms of heat and momentum addition) to the subsonic and supersonic regions of the wind (Section 3). Having indicated a possible need for outward energy transport from the coronal base by some means other than advection or thermal conduction, we shall consider the propagation of hydromagnetic waves in the solar atmosphere and solar wind and the role such waves might play in transporting the additional energy (Section 4). Finally, we shall discuss the specific acceleration mechanism involving Alfvén waves interacting with the solar wind – this being both the most thoroughly studied and conceptually the simplest energy addition mechanism (Section 5). The extension of this mechanism to the description of massive winds from cool, low-gravity stars will be briefly outlined in Section 6, and a few closing remarks will be presented in Section 7.

2. Thermally Driven Solar Wind

Our present understanding of the solar wind is based on the work of Parker (1958, 1960, 1963, 1964a, b, 1965). His first solar wind paper (Parker, 1958) dealt with the spherically symmetric expansion of an isothermal corona and provided a sound physical description of the dynamical effects important in the accelaration of the solar wind. Parker (1963, 1964a, b, 1965) later extended this work to include the effects of non-spherical flow and of energy balance in the coronal expansion. The latter work concentrated on classical thermal conduction in a spherical expansion, but the effects of non-classical conduction and energy addition above the coronal base were also considered. In light of observations that have become available over the past 15-y, several other workers have expanded on this theoretical basis and clarified the roles that the physical effects discussed by Parker play in the acceleration of the solar wind. In reviewing our present understanding of this subject, we shall begin with the case of a thermally driven solar wind: that is, a wind in which the driving force is the thermal pressure gradient force and the retarding force results from the solar gravitational field.

There have been several approaches taken toward describing a thermally driven solar wind, ranging from the original isothermal model to conductive, viscous, one-fluid and

two-fluid models (for references to this work see reviews by Holzer and Axford (1970), Hundhausen (1972), Barnes (1975), Hollweg (1978a), Holzer (1979)). To illustrate the physical effects that are important in a thermally driven wind, we shall discuss results from inviscid, one-fluid models including various descriptions of thermal conduction and both spherical and more rapidly expanding flow geometries. We use inviscid, one-fluid models because viscosity is negligible, except in the vicinity of steep velocity gradients (Parker, 1963), and because two-fluid models do not provide additional information that would be of interest in the following discussion. Rapidly expanding flow geometries must be considered because they seem to be characteristic of coronal holes, in which the magnetic field diverges rapidly (e.g. Altschuler *et al.*, 1972; Munro and Jackson, 1977), and the flow is expected to follow the field near the Sun. The equations for mass, momentum, and energy balance which we shall use to describe the steady, radial flow of this thermally driven electron-proton solar wind are thus

$$nmuA = \mathcal{F} = \text{const.} \tag{1}$$

$$u \frac{\mathrm{d}u}{\mathrm{d}r} = -\frac{1}{nm} \frac{\mathrm{d}p}{\mathrm{d}r} - \frac{GM}{r^2}, \tag{2}$$

$$3nuk \frac{\mathrm{d}T}{\mathrm{d}r} = 2ukT \frac{\mathrm{d}n}{\mathrm{d}r} - \frac{1}{A} \frac{\mathrm{d}}{\mathrm{d}r}(qA), \tag{3}$$

where A is the cross-sectional area of an infinitesimal, radial flow tube, n is the electron (proton) number density, m is the proton mass, u is the radial flow speed, T is half the sum of the electron and proton temperatures, $p = 2nkT$, q is the radial heat flux density, and k, G, and M are the Boltzmann constant, gravitational constant, and solar mass. An alternative form for the energy balance equation is

$$\mathcal{F}\left(\tfrac{1}{2}u^2 + 5\frac{kT}{m} - \frac{GM}{r} + \frac{A}{\mathcal{F}} q\right) = F = \text{const.} \tag{4}$$

If the magnetic field is radial, and the solar wind plasma is assumed to be collision-dominated, the heat flux density can be described classically (Spitzer, 1962) by

$$q = q_a = -\kappa_0 T^{5/2} \frac{\mathrm{d}T}{\mathrm{d}r}, \tag{5}$$

where $\kappa_0 = 7.8 \times 10^{-7}$ erg cm^{-1} s^{-1} K$^{-7/2}$. If account is taken of the spiral shape of the interplanetary magnetic field (Parker, 1958) and of the strong inhibition of thermal conduction across the magnetic field (e.g., Chapman and Cowling, 1939), then the heat flux density takes the form (Parker, 1964b).

$$q = q_b = q_a \cos^2\theta, \tag{6}$$

where θ is the angle between the radial direction and the local magnetic field. Of course, the solar wind plasma is not collision-dominated, except, perhaps, relatively near the Sun, and the classical description of thermal conduction must be modified (e.g., Parker, 1964b; Perkins, 1973). Hollweg (1976) has suggested that in a collisionless solar wind plasma the heat flux density can be represented by

$$q = q_c = \tfrac{3}{2}\alpha nukT, \tag{7}$$

where α is an arbitrary parameter, which will be taken here to be 4. Hollweg (1976) represents q by (6) when the mean free path of a thermal electron is less than half the radial distance and by (7) otherwise. Recently, Scudder and Olbert (1979a, b) have derived a kinetic description (including Coulomb collisions) of solar wind electrons, and their results indicate that the solar wind heat flux may not be adequately described by any of the above models. Although detailed calculations relevant to acceleration of the solar wind are not yet available, we shall make use of existing information (Olbert, 1981) to discuss (later in this section) the possible implications of this kinetic description for a thermally driven wind.

Durney (1972) obtained numerical solutions to (1)–(3) and (5) for spherical symmetry ($A \sim r^2$), and some of these are displayed in Figure 2a to illustrate the dependence of particle flux density and flow speed at 1 AU ($n_E u_E$ and u_E) on the coronal base density (n_0) and temperature (T_0). We see that the particle flux density ($n_E u_E$) increases rapidly with increasing T_0, if n_0 is fixed. Similarly, for $n_0 \lesssim 10^7$ cm^{-3}, the solar wind flow speed (u_E) increases as T_0 increases, but for $n_0 \gtrsim 10^8$ cm^{-3}, u_E decreases with increasing T_0. It is worth spending a little time trying to understand this behavior of $n_E u_E$ and u_E, for by doing this we can lay a basis for understanding all the important physical effects (associated with accelerating the solar wind) that we shall consider in the remainder of the paper.

Let us first consider the dependence of the solar wind mass flux on coronal temperature (cf. Parker, 1958, 1964a). For an isothermal corona, (2) is readily integrated from the coronal base ($r = r_0$) to the critical point ($r = r_c = GMm/4\beta_c kT$, where $\beta = (r/2A)\,(\mathrm{d}A/\mathrm{d}r)$) to yield the flow speed at the coronal base (Leer and Holzer, 1979)

$$u_0 = \left(\frac{2kT}{m}\right)^{1/2} \left(\frac{r_c}{r_0}\right)^2 f_c \exp\left\{-\left[\frac{GMm}{2kTr_0} + \tfrac{1}{2} - 2\beta_c\right]\right\} \tag{8}$$

where $f = r_0^2 A/r^2 A_0$, and we assume $u_0^2 \ll 2kT/m$. Because $n_E u_E \propto u_0$, it is clear that for a strongly gravitationally bound corona ($GM/r_0 \gg 2kT/m$) the solar wind mass flux ($\propto n_E u_E$) is dominated by the exponential coronal temperature dependence shown in (8). Hence, a small increase in coronal temperature produces a large increase in solar wind mass flux. (The isothermal assumption is not especially restrictive in the above analysis, for T can be taken to represent an average coronal temperature in the region of subsonic solar wind flow (Leer and Holzer, 1979)).

If our physical intuition were based entirely on polytropic (including isothermal) models of the solar wind, we would immediately conclude that this strong dependence

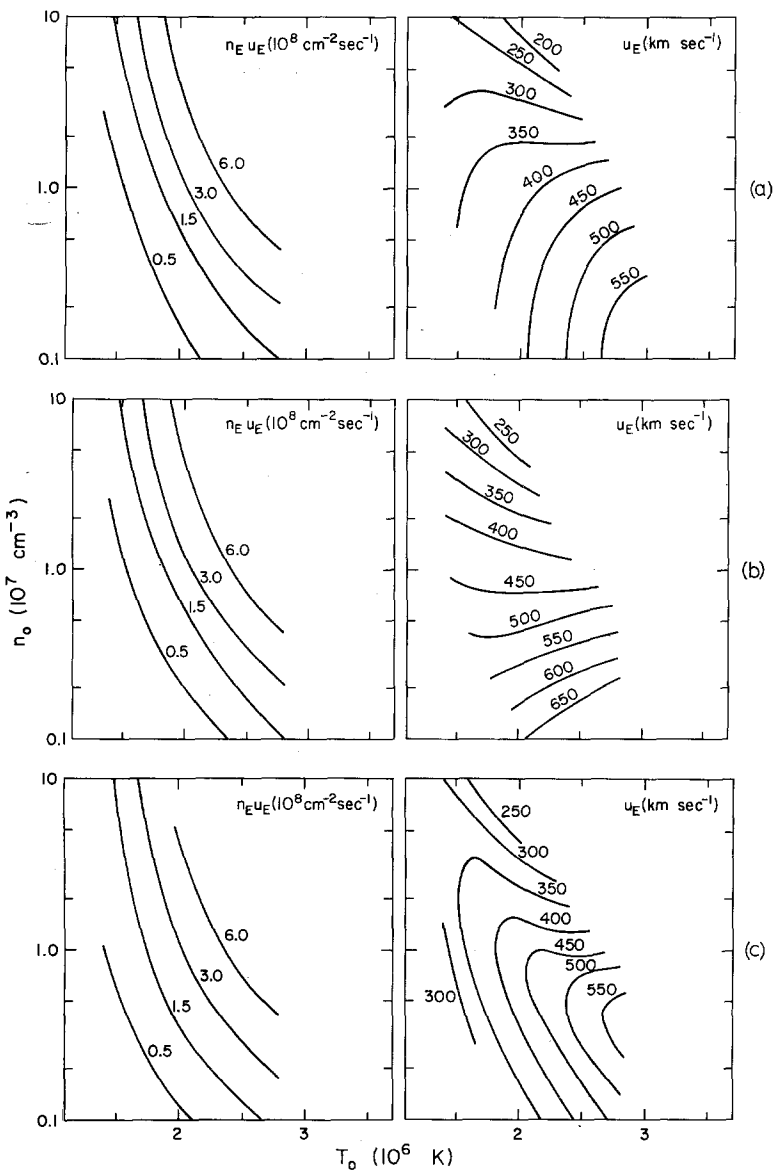

Fig. 2. Contours of constant particle flux density at 1 AU ($n_E u_E$) and flow speed at 1 AU (u_E) shown in the $n_0 - T_0$ plane (where n_0 and T_0 are the coronal base density and temperature) for the spherically symmetric flow of a conductive, thermally driven wind: (a) Durney's (1972) solutions for a classical (collision-dominated) conduction law; (b) solutions of Durney and Hundhausen (1974) for magnetically inhibited thermal conduction; solutions for the collisionlessly inhibited thermal conduction description used by Hollweg (1976) (from Holzer and Leer, 1980).

of mass flux on coronal temperature has no effect on the solar wind flow speed (u_E), because the mass flux scales out of polytropic representations (e.g. Parker, 1964a; Hundhausen, 1972). In fact, the same sort of scaling occurs when T is specified as a function of r ($T = T_0 \Theta(r)$): in either case, u_E depends only on T_0. If, however, a proper

energy equation (e.g., (3)) is considered, it is clear that the magnitude of the mass flux determines the relative importance of thermal conduction and, say, expansive cooling. In Durney's (1972) model, when the mass flux is small (viz., for $n_0 \lesssim 10^7\ \mathrm{cm}^{-3}$) conduction dominates everywhere, and the relevant solution of (3) is $T = T_0(r_0/r)^{2/7}$ (Parker, 1964a; Chapman, 1957). As noted above, this case, like the polytropic case, leads to a monotonic increase of u_E with increasing T_0, owing to the increasing strength of the pressure gradient force with increasing T_0. Yet, for larger mass fluxes, conduction ceases to dominate in certain domains, and expansive cooling leads to a more rapid temperature decline and a consequent decrease in efficiency of acceleration of the flow by the pressure gradient force. If the base density and temperature are large enough (e.g., $T_0 \gtrsim 1.5 \times 10^6$ at $n_0 \approx 10^8\ \mathrm{cm}^{-3}$ or $T_0 \gtrsim 2 \times 10^8$ K at $n_0 \approx 2 \times 10^7\ \mathrm{cm}^{-3}$), the expansive cooling is so effective that conduction is unimportant at $r = r_E = 1$ AU, and virtually all of the solar wind energy flux at 1 AU is carried by the flow. In this case, (4) can be evaluated at the coronal base and at 1 AU to yield

$$F/\mathscr{F} \approx u_E^2/2 \approx q_0 A_0/\mathscr{F} + 5kT_0/m - GM/r_0\,. \tag{9}$$

Now we can understand why Durney's results (Figure 2a) indicate that u_E decreases as T_0 increases, when n_0 and T_0 are large enough: the heat flux density at the coronal base (q_0) does not increase as rapidly with T_0 ($q_0 \propto T_0^{7/2}$) as does the mass flux ($\mathscr{F} \propto u_0$; cf. (8)), so the conductive energy per unit mass ($q_0 A_0/\mathscr{F}$) decreases more rapidly than the enthalpy per unit mass ($5kT_0/m$) increases, and the total energy per unit mass supplied to the solar wind ($F/\mathscr{F} \approx u_E^2/2$) decreases.

This line of argument is especially important for what follows, because it is clear from solar wind observations (e.g. Hundhausen, 1972) that $F/\mathscr{F} \approx u_E^2/2$ (i.e., at 1 AU the solar wind energy flux is transported almost entirely by the flow). Hence, if we can determine the outward energy flux in the corona (F) and the resulting mass flux ($\mathscr{F}$), we then know (for realistic models) what the flow speed at 1 AU must be ($u_E \approx \sqrt{2F/\mathscr{F}}$).

Let us turn next to the model of Durney and Hundhausen (1974), in which inhibition of the radial heat flux by the spiral interplanetary magnetic field is considered (i.e., (1)–(3) and (6) are solved). Some results of this model are shown in Figure 2b, and comparison with Figure 2a indicates that the solar wind mass flux is only slightly affected by the conduction inhibition, but the flow speed at 1 AU is increased significantly over a broad range of values of n_0 and T_0. The principal effect of inhibition of thermal conduction in a *strongly conduction-dominated* solar wind flow is the establishment of a temperature plateau, a region of elevated temperature extending from the coronal base out to the distance (in this case, several tens of solar radii) where the inhibition becomes effective (e.g. Parker, 1964b; Durney and Hundhausen, 1974). This temperature plateau has little effect on the average temperature in the region of subsonic flow and thus little effect on the mass flux, but it significantly enhances the pressure gradient in the supersonic region and thus leads to a higher-speed solar wind. In terms of energy balance, one can say that this inhibition reduces the conduction flux at the coronal base, but substantially increases the efficiency with which the conduction flux is transformed to flow energy (through the pressure gradient force), resulting in a net

increase in the energy flux supplied to the flow at 1 AU. Together with only a modest change in the mass flux, this leads to an increase in the flow energy per unit mass ($u_E^2/2$). A notable feature of Figure 2b (see also Figure 2a) is the monotonic decrease of u_E with increasing n_0. This results from the fact that the mass flux depends more strongly on base density than do either the conduction flux density at the base or the efficiency of conversion from conductive to flow energy, so that the energy per unit mass supplied to the flow is decreased when n_0 is increased (Holzer and Leer, 1980).

The only substantive difference between the magnetic inhibition of conduction discussed by Durney and Hundhausen (1974) and the collisionless inhibition discussed by Hollweg (1976) (see Figure 2c) is that the latter inhibition can take place much nearer the Sun and can more strongly inhibit the conduction. For very low base densities, electrons in the coronal plasma are collisionless everywhere above the coronal base, and in Hollweg's (1976) model $q = q_c$ everywhere, so that the flow is polytropic (cf. (7)). For low to moderate densities, however, the electrons are assumed collision-dominated near the Sun (i.e., $q = q_b$), and the point where the conduction is inhibited (i.e., where the plasma is assumed to become collisionless and q becomes q_c) moves rapidly away from the Sun with increasing n_0. The resulting increase in conduction flux with increasing n_0 is more rapid than the increase in mass flux, and given the uniformly high efficiency of conversion from conduction energy to flow energy associated with collisionless inhibition, the energy per unit mass supplied to the flow ($u_E^2/2$) increases (Holzer and Leer, 1980). This effect is seen in the lower left portion of the n_0–T_0 plane shown in Figure 2c, where u_E increases with increasing n_0.

It is clear from Figure 2 that high speed solar wind streams, in which $u_E > 600$ km s^{-1} and $n_E u_E \approx 3 \times 10^8$ cm^{-2} s^{-1} (e.g., Feldman *et al.*, 1977), cannot be produced in these three conductive models unless n_0 is taken to be unrealistically low. (Withbroe (1977) indicates that $n_0 T_0 \gtrsim 10^{14}$ cm^{-3} K, which implies $n_0 \gtrsim 5 \times 10^7$ cm^{-3}.) We then must ask whether the rapidly diverging flow expected in solar coronal holes can lead to a substantial increase in u_E for the same three types of conductive model. This question has been addressed by Holzer and Leer (1980), who have extended the models of Durney (1972), Durney and Hundhausen (1974), and Hollweg (1976) to include the effects of rapidly diverging flow geometries. Figure 3 shows their results for a flow geometry described by (Kopp and Holzer, 1976):

$$A = A_0 (r/r_0)^2 f\,, \tag{10}$$

$$f = (f_{\max} e^{(r-r_1)/\sigma} + f_1)/(e^{(r-r_1)/\sigma} + 1)\,, \tag{11}$$

$$f_1 = 1 - (f_{\max} - 1)\, e^{(r_0 - r_1)/\sigma}\,, \tag{12}$$

with $\sigma = 0.1 R_\odot$, $r_1 = 2R_\odot$, and $f_{\max} = 7$. Here, σ measures the radial scale over which a flow tube expands faster than it would in a spherical geometry, r_1 indicates the radial location where the rapid expansion occurs, and $f_{\max}$ is the ratio as $r \to \infty$ of the area of a rapidly expanding flow tube to that of a spherically expanding flow tube, when their areas are equal at $r = r_0$. In the chosen flow geometry, three critical points may exist, and in some cases the only acceptable solution exhibits a shock transition between the

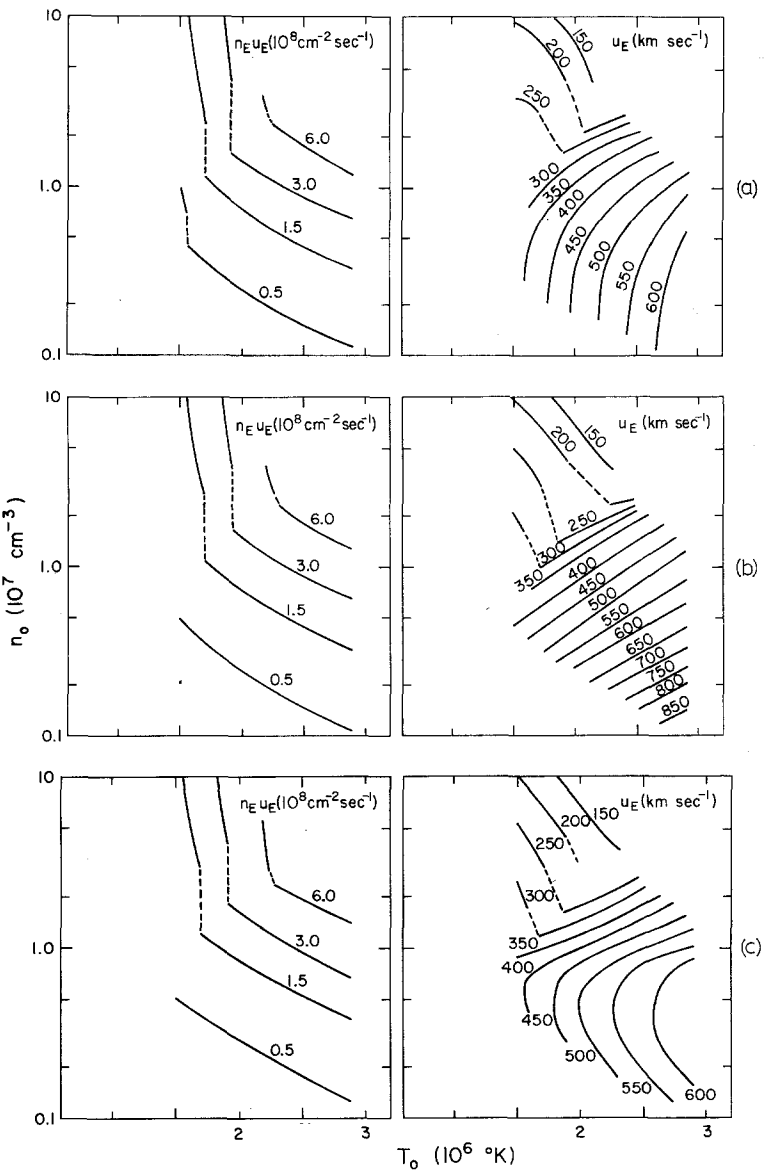

Fig. 3. Same as Figure 2, except for a rapidly diverging flow instead of a spherically symmetric flow. The flow geometry is characterized by $\sigma = 0.1R_\odot$, $r_1 = 2R_\odot$, and $f_{max} = 7$, which means that the flow tube area increases by a factor of 7 more than in the spherical case, and most of the rapid area increase takes place in $1.9R_\odot \lesssim r \lesssim 2.1R_\odot$. The dashed lines indicate regions where a shock transition exists somewhere between the inner and outer critical points (cf. Figure 5a and Holzer (1977)) (from Holzer and Leer, 1980).

inner and outer critical points (Holzer, 1977; Habbal and Tsinganos, 1982). Such solutions were not calculated in this study, but their region of existence is indicated by the dashed lines in Figure 3. It is found that a rapidly expanding flow geometry leads to a slightly higher mass flux density at the coronal base, but a slightly lower mass flux

density at 1 AU. The solar wind flow speed is also modified somewhat, but the basic conclusion drawn from the spherically symmetric studies remains unchanged: conductive solar wind models in which the heat flux is described by (5), (6), or (6) and (7) cannot explain the existence of the observed high-speed solar wind streams.

There remains the possibility (Olbert, 1981) that a more realistic description of thermal conduction, like the one being worked out by Scudder and Olbert (1979a, b), will allow high-speed streams to be produced in a conductive model without energy addition above the coronal base. In order to satisfy observational constraints on the coronal pressure and the solar wind mass flux density and flow speed at 1 AU, it appears that such a description will have to lead to a coronal temperature that is higher in at least part of the region of supersonic flow than the average temperature in the subsonic region. Whether such a temperature profile is consistent with the kinetic description of Scudder and Olbert remains to be seen. For the time being, we shall assume that high-speed streams require energy addition to the solar wind above the coronal base (by some means other than degradation of the heat flux).

3. Energy Addition

A general discussion of energy addition above the coronal base requires that our descriptions of momentum and energy balance (cf. (2)–(4)) be modified as follows:

$$u \frac{\mathrm{d}u}{\mathrm{d}r} = -\frac{1}{nm}\frac{\mathrm{d}p}{\mathrm{d}r} - \frac{GM}{r^2} + D\,, \tag{13}$$

$$3nuk \frac{\mathrm{d}T}{\mathrm{d}r} = 2ukT \frac{\mathrm{d}n}{\mathrm{d}r} - \frac{1}{A}\frac{\mathrm{d}}{\mathrm{d}r}(qA) + Q\,, \tag{14}$$

$$\mathscr{F}\left(\tfrac{1}{2}u^2 + 5\frac{kT}{m} - \frac{GM}{r} + \frac{A}{\mathscr{F}}q\right) = F = F_0 + \int_{r_0}^{r} \mathrm{d}r'\,(D\mathscr{F} + AQ)\,, \tag{15}$$

where nmD and Q are the rates (per volume, per time) at which momentum and heat are added to the plasma. The momentum addition can be thought of as the application of an outward-directed body fore per unit mass, D. An energy flux associated with both the heat and momentum addition can be defined by

$$\Delta F = \int_0^{\infty} \mathrm{d}r(D\mathscr{F} + AQ)\,, \tag{16}$$

and this will prove a useful parameter in the following discussion of the effects of energy addition on the solar wind particle flux density, flow speed, and temperature at 1 AU ($n_E u_E$, u_E, and T_E). In this discussion, we shall find it instructive to consider heat addition and momentum addition separately.

Let us begin with heat addition, setting $D = 0$ and writting

$$Q = Q_{i\exp}\left[-100\left(\frac{r}{r_i}-1\right)^2\right]. \tag{17}$$

(17) describes the heating of the solar wind in a narrow region centered at $r = r_i$ and allows us to study the effects of adding heat at various locations in the flow by solving (1), (13), (14), and (17) for several values of r_i ranging from $r_i = r_0$ to $r_i \gtrsim 1$ AU. The magnitude of the heating can be specified in such a study by requiring that the energy flux added to the wind be independent of the location where the energy is added: i.e., $(\partial/\partial r_i)(\Delta F) = 0$. Because of our desire to match as closely as possible the observation (e.g. Hundhausen, 1972) that $F_E/\mathscr{F} \approx u_E^2/2$, we shall use Hollweg's (1976) representation of thermal conduction (cf. Section 2), in which the plasma is assumed collision-dominated ($q = q_b$: see (6)) wherever the mean free path of thermal electrons is less than half the radial distance, and it is assumed collisionless ($q = q_c$: see (7)) otherwise. The difficulty with the classical description of thermal conduction ($q = q_a$ everywhere) is that frequently $q_E A_E/\mathscr{F} \gtrsim u_E^2/2$, and a significant fraction of the energy flux added by heating above the coronal base is carried past 1 AU by an enhanced thermal conduction flux, causing the predicted flow speed (u_E) to be unrealistically low (see the results of Pneuman (1980) for an example of this difficulty).

The above model (with collisionless inhibition of conduction) has been studied by Leer and Holzer (1980) for spherically symmetric flow, and their results are shown in Figure 4a. Coronal base parameters are taken to be $n_0 = 10^8\ \mathrm{cm}^{-3}$ and $T_0 = 1.4 \times 10^6$ K, and the magnitude of the heat addition is prescribed by $\Delta F/F_R = 0$, 0.3, and 1 in the three cases shown. The reference energy flux, F_R, is the solar wind energy flux ($F = F_0$) in the absence of energy addition above the coronal base ($\Delta F = 0$), and it generally differs from the coronal base energy flux (F_0) in the presence of energy addition ($\Delta F \neq 0$). The critical (sonic) point of the flow occurs near $10R_\odot$ in the reference case ($\Delta F = 0$), but moves inward (as far as $4R_\odot$ for $\Delta F = 1$) when heat is added to the subsonic flow. The addition of heat in the subsonic region increases the local temperature and thus increases the mass flux ($\mathscr{F} \propto n_E u_E$). This mass flux increase very nearly balances the increase in energy flux (ΔF), so the flow speed at 1 AU ($u_E \approx \sqrt{2F_E/\mathscr{F}}$) is not significantly changed. When, however, heat is added in the supersonic region, the temperature in the subsonic region is generally unaffected, and the mass flux ($\mathscr{F}$) is unchanged; the increase in energy flux (ΔF) thus leads to an increase in the flow speed at 1 AU ($u_E \approx \sqrt{2F_E/\mathscr{F}}$). As the location of the heat addition moves farther out in the solar wind, there is less time before the wind reaches 1 AU for the conductive energy and internal energy to be converted into flow energy through the action of the pressure gradient force. As a result, T_E increases and u_E decreases as r_i increases (in the supersonic region); evidently, if heat is added too far out in the wind, the temperature at 1 AU can become unrealistically large. (The decrease in u_E below its reference value when $r_i \approx 1$ AU results from the localized inward pressure gradient force associated with the spatially narrow heating function used here.) Quite similar

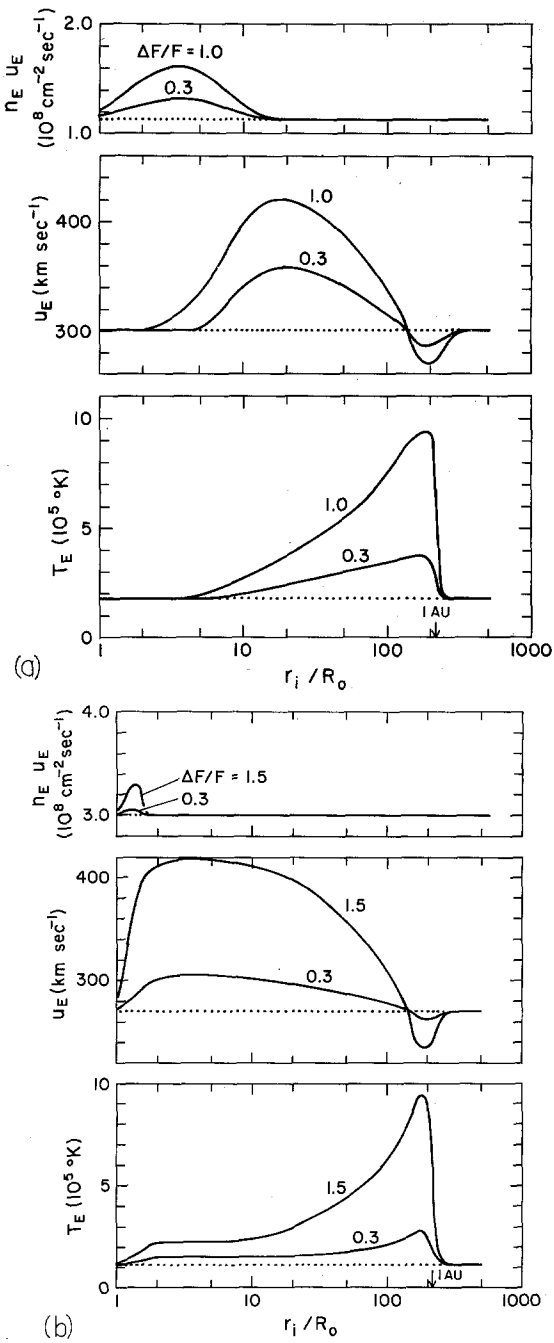

Fig. 4. Values at 1 AU of the proton flux density ($n_E u_E$), flow speed (u_E), and temperature (T_E) for a range of locations (r_i) of a spatially narrow heat addition function: (a) spherically symmetric flow, with $n_0 = 10^8$ cm^{-3} and $T_0 = 1.4 \times 10^6$ K; (b) rapidly diverging flow ($f_{\max} = 7$, $\sigma = 0.1 R_\odot$, $r_1 = 2R_\odot$), with $n_0 = 1.6 \times 10^7$ cm^{-3} and $T_0 = 2.5 \times 10^8$ K. The dotted lines indicate the reference values of parameters (i.e., values for $\Delta F = 0$) and the solid lines correspond to (a) $\Delta F/F_R = 0.3, 1.0$ and (b) $\Delta F/F_R = 0.3, 1.5$. The sonic (critical)point in the reference models ($\Delta F = 0$) is near $10R_\odot$ in (a) and near $1.8R_\odot$ in (b) (from Leer and Holzer, 1980).

results are found for a rapidly expanding flow geometry (Figure 4b): heat addition in the subsonic region increases the solar wind mass flux, but has little effect on the flow speed at 1 AU; heat addition in the supersonic region does not affect the mass flux, but increases the flow speed at 1 AU. Of course, in the rapidly expanding flow geometry, the sonic point lies much nearer the Sun, so u_E can be increased with heat addition much nearer the Sun than in the spherically symmetric models.

Now let us consider the effects of momentum addition, setting $Q = 0$ and writing (cf. (17))

$$D = D_i(A/A_i) \exp\left[-50\left(\frac{r}{r_i} - 1\right)^2 \right]. \tag{18}$$

Solutions to (1), (13), (14), and (18) are shown in Figure 5a and b for spherical and rapidly expanding flow geometries and the same model parameters as used in the heat addition study (Figure 4) (Leer and Holzer, 1980). The dashed lines in Figure 5a indicate solutions (not calculated) in which shocks occur between the inner and outer critical points (cf. Figure 3). As in the case of heat addition, energy addition by direct acceleration (momentum addition) leads to an enhanced mass flux when the energy is added in the region of subsonic flow, but not when it is added in the supersonic region. The mass flux enhancement, however, is somewhat larger when a given amount of energy is added as momentum (Figure 5) than when the same amount of energy is added as heat (Figure 4). When all the energy is added between the coronal base and the (innermost) critical point (at $r = r_c$), the increase in mass flux ($\mathscr{F} - \mathscr{F}_R$) over the reference model mass flux ($\mathscr{F}_R$) is represented approximately by

$$\mathscr{F} \approx \mathscr{F}_R \exp(mI/2k \langle T \rangle). \tag{19}$$

where $I = \int_{r_0}^{r_c} dr\, D$, and $\langle T \rangle$ is the average subsonic-region temperature (Leer and Holzer, 1979). The increase in mass flux resulting from momentum addition in the subsonic region is due to the increased velocity scale height and the inward motion of the critical point, which are characteristic consequences of momentum addition, heat addition, or increased coronal base temperature.

Because the addition of energy by direct acceleration (momentum addition) in the subsonic region leads to an enhancement of the mass flux that is significantly larger than that associated with the addition of the same amount of energy by heating, it is not surprising that momentum addition in the subsonic region leads to a substantial decrease in flow speed at 1 AU (see u_E in Figures 5a and b). As with heat addition, the addition of momentum in the supersonic region increases u_E (again, because $\mathscr{F}$ is unchanged and F_E is increased), but the momentum addition is more uniformly efficient in increasing u_E (cf. Figures 4 and 5), because adding momentum has little effect on the temperature profile, and virtually all of the energy flux at 1 AU is carried as flow energy, regardless of how near 1 AU the momentum is added. In fact T_E is generally decreased by momentum addition, either because of an increased expansive cooling (for addition in the supersonic region) or because of an inward movement of the point at which inhibition of thermal conduction occurs (for addition nearer the Sun).

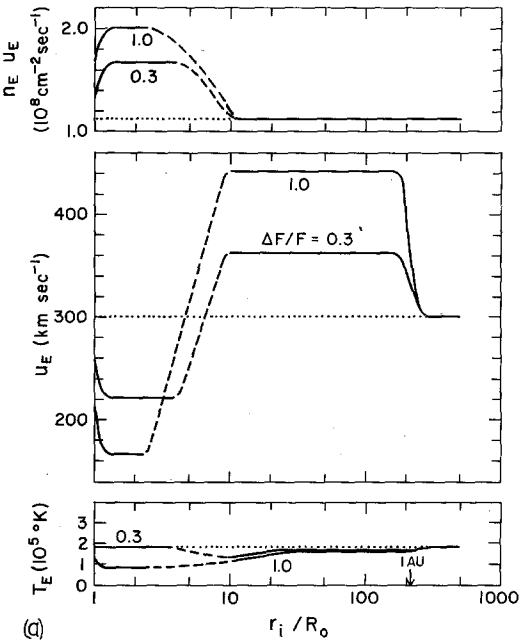

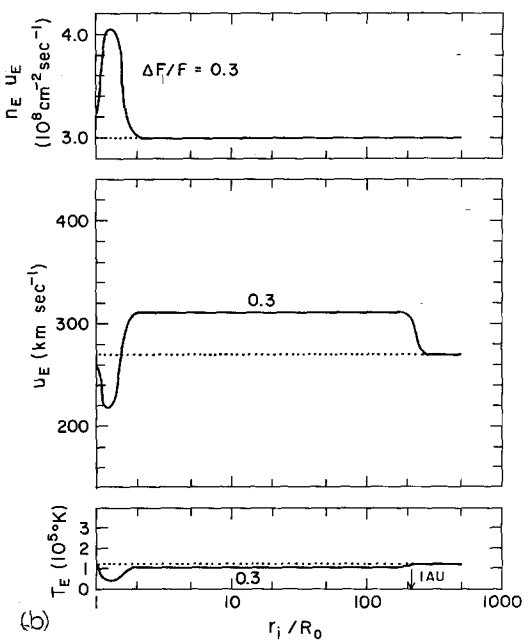

Fig. 5. Same as Figure 4, but for momentum addition instead of heat addition. The dashed portions of the curves in Figure 5a indicate solutions passing through an inner critical point, shocking to subsonic flow, and then passing through an outer critical point, beyond which the flow remains supersonic (cf. Figure 3 and Holzer (1977)) (from Leer and Holzer, 1980).

Two other aspects of the general energy addition problem that are of interest here are momentum loss in the subsonic region and energy exchange between the subsonic and supersonic regions (see Leer and Holzer (1980) for a detailed discussion). As can be inferred from Figure 5, momentum loss (i.e., an additional inward-directed force that decelerates the flow) should decrease the solar wind mass flux and increase the flow speed at 1 AU. This effect has been demonstrated for the frictional force associated with a substantial, but not unreasonable, abundance of $He^{+\,+}$ in the corona (Leer and Holzer, 1979), and it is conceivable that some other type of inward force, perhaps electromagnetic in nature, might be effective in the subsonic region. One can also infer from Figures 4 and 5 that any process whereby energy is removed from the subsonic region and deposited in the supersonic region will lead to a decrease in the solar wind mass flux and an increase in the flow speed at 1 AU. Such a process might involve the generation of, say, hydromagnetic waves in the subsonic region and their propagation into and dissipation in the supersonic region.

It is clear from the above discussion that an energy flux (other than advective or conductive) emanating from the coronal base will be most effective in producing high-speed solar wind streams if it is deposited in the solar wind in the region of supersonic flow. There may, however, be no need for such an energy flux if there exists a process which removes momentum from (decelerates the flow in) the subsonic region or which removes energy from the subsonic region and redeposits it in the supersonic region.

4. Alfvén Waves in the Solar Atmosphere

We have indicated that it may be necessary to add energy to the solar wind above the coronal base to accelerate high-speed streams. Hydromagnetic waves represent one means whereby this energy might be transported from the lower solar atmosphere to the region in the solar wind where it is deposited, and Alfvénic fluctuations observed at 1 AU (Belcher and Davis, 1971) could well represent remmants of such a transport process. Fast-mode and slow-mode hydromagnetic waves have a compressional component and generally suffer stronger damping than Alfvén waves (e.g. Barnes, 1979), so even if a substantial energy flux in all three modes were present in the corona, one would expect to see the remnant energy flux only in the Alfvén mode at 1 AU. In this section and the following section, we shall concentrate on the transport of energy by Alfvén waves in the solar atmosphere and the solar wind, not because Alfvén waves are more likely to be important than fast-mode and slow-mode waves, nor because energy transport by means other than hydromagnetic waves is unlikely, but because Alfvén waves are the most thoroughly studied energy transport mechanism, and we can gain a good bit of general understanding of energy transport through a careful consideration of Alfvén waves.

Hydromagnetic waves may be generated in the corona (e.g., Barnes, 1969), or they may be generated in the lower solar atmosphere and propagate into the corona. In the latter case, propagation through the transition region (between the chromosphere and

corona) involves certain difficulties (e.g. Osterbrock, 1961): fast-mode waves are refracted strongly and can carry no significant energy flux through the transition region, into the corona; slow-mode waves steepen rapidly in the transition region (if they are not already shocks in the upper chromosphere) and the resulting shock waves dissipate their energy below or very near the coronal base. In addition, observations of solar oscillations in the middle chromosphere (Athay and White, 1979a) place a lower limit on the upward energy flux density carried by slow-mode waves of about 2×10^4 erg cm^{-2} s^{-1} and an upper limit of about 10^5 erg cm^{-2} s^{-1} (Athay and White, 1979b), which is much less than the energy flux density required to heat the corona and drive the solar-wind in coronal holes ($\approx 5 \times 10^5$ erg cm^{-2} s^{-1}), to say nothing of that required to heat the upper chromosphere. These observations (Athay and White, 1979a, b) can also be used to place limits on the energy flux carried by Alfvén waves, but a careful analysis of the behavior of Alfvénic disturbances in the lower solar atmosphere must first be carried out, and this is done below.

Because of the very small density scale-height in the lower solar atmosphere, a moderate wave period (min to h) of an Alfvénic disturbance is comparable to or longer than an Alfvénic travel-time across a characteristic scale-length of the medium (i.e., $\omega \lesssim \mathrm{d}v_A/\mathrm{d}s$, where ω is the disturbance frequency and v_A the Alfvén speed), so the WKB approximation, normally used to describe Alfvén-wave propagation, breaks down. Analysis of Alfvénic disturbances, therefore, requires a reconsideration of the conservation laws and Maxwell's equations. For slow oscillations of the plasma in the solar atmosphere, the mass and momentum conservation laws, Ampère law, and Faraday's law can be written

$$\frac{\partial \rho}{\partial t} + \nabla \cdot \rho \mathbf{u} = 0 , \tag{20}$$

$$\rho\left(\frac{\partial}{\partial t} + \mathbf{u} \cdot \nabla\right)\mathbf{u} = -\nabla p - \rho \frac{GM}{r^2} \hat{e}_r + \mathbf{j} \times \mathbf{B}/c , \tag{21}$$

$$\nabla \times (\mathbf{E} + \mathbf{u} \times \mathbf{B}/c) = 0 , \tag{22}$$

$$\nabla \times \mathbf{B} = \frac{4\pi}{c} \mathbf{j} , \tag{23}$$

$$\nabla \times \mathbf{E} = -\frac{1}{c} \frac{\partial \mathbf{B}}{\partial t} , \tag{24}$$

where $\rho = nm$. Let us consider toroidal Alfvénic disturbances in an axisymmetric background plasma. First, (20)–(24) yield two equations for the ϕ components (in

spherical coordinates) of **u** and **B**:

$$\rho\left(\frac{\partial}{\partial t} + \mathbf{u}\cdot\nabla\right)u_\phi + \frac{\rho u_\phi}{r}(u_r + u_\theta \tan\theta) + \frac{1}{r\sin\theta}\frac{\partial p}{\partial \phi} =$$

$$= -\frac{1}{4\pi}\left[\frac{1}{2r\sin\theta}\frac{\partial B^2}{\partial \phi} - \right.$$

$$\left. - (\mathbf{B}\cdot\nabla)B_\phi - \frac{B_\phi}{r}(B_r + B_\theta \cot\theta)\right], \tag{25}$$

$$\left(\frac{\partial}{\partial t} + \mathbf{u}\cdot\nabla\right)B_\phi + \frac{u_\phi}{r}(B_r + B_0\cot\theta) =$$

$$= (\mathbf{B}\cdot\nabla)u_\phi + \frac{B_\phi}{r}(u_r + u_0\cot\theta) -$$

$$- B_\phi\left(\frac{\partial}{\partial t} + \mathbf{u}\cdot\nabla\right)\ln\rho\,. \tag{26}$$

Now, if we assume axial symmetry ($\partial/\partial\phi = 0$), take the background flow velocity and magnetic field to be radial ($u_\theta = B_0 = 0$), and assume that terms of second order in the disturbance quantities ($\delta v = u_\phi$, $\delta B = B_\phi$) can be neglected (allowing the neglect of $\partial\rho/\partial t$), we find, following Heinemann and Olbert (1980), that in the limit $\sqrt{u} \ll \sqrt{v_A}$

$$\left(\frac{\partial}{\partial t} - v_A\frac{\partial}{\partial r}\right)f = -\tfrac{1}{2}g\frac{dv_A}{dr}, \tag{27}$$

$$\left(\frac{\partial}{\partial t} + v_A\frac{\partial}{\partial r}\right)g = \tfrac{1}{2}f\frac{dv_A}{dr}, \tag{28}$$

where $\delta v = \delta v_0(\rho_0/\rho)^{1/4}(g-f)/(g_0-f_0)$, $\delta B = \delta B_0(\rho/\rho_0)^{1/4}(g+f)/(g_0+f_0)$, and $v_A^2 = B_r^2/4\pi\rho$.

If $f, g \propto \exp(-i\omega t)$, then (27) and (28) have simple solutions in the two limits $\omega \ll v_A'$ and $\omega \gg v_A'$ (where $v_A' = dv_A/dr$). In the low-frequency limit ($\omega \ll v_A'$) the first term on the left side in both (27) and (28) is negligible, and we have the two solutions

$$f_\pm = \pm g_\pm = f_0\left(\frac{v_A}{v_{A0}}\right)^{\pm 1/2} e^{-i\omega t}, \tag{29}$$

$$\delta v_- = \delta v_0\left(\frac{r}{r_0}\right)e^{-i\omega t}, \tag{30}$$

$$\delta B_- = \delta B_0 \left(\frac{r_0}{r}\right) \left(\frac{v_{A0} v'_{A0}}{v_A v'_A}\right) e^{-i\omega t} =$$

$$= -i\delta v_- \left(\frac{B_r}{2v_A}\right) \left(\frac{\omega}{v'_A}\right) = 0\left(\frac{\omega}{v'_A}\right), \tag{31}$$

$$\delta v_+ = \delta v_0 \left(\frac{r}{r_0}\right) \frac{\ln (\omega/v'_A)}{\ln (\omega/v'_{A0})} e^{-i\omega t} =$$

$$= i\delta B_+ \left(\frac{v_A}{B_r}\right) \left(\frac{\omega}{v'_A}\right) \ln\left(\frac{\omega}{v'_A}\right) = 0\left(\frac{\omega}{v'_A}\right) \tag{32}$$

$$\delta B_+ = \delta B_0 \left(\frac{r_0}{r}\right) \left(\frac{v'_A v_{A0}}{v_A v'_{A0}}\right) e^{-i\omega t}. \tag{33}$$

These solutions have a straightforward physical interpretation: if a toroidal oscillation is imposed on the atmosphere at $r = r_1$, the first $(-)$ solution describes the rigid-body oscillation of the lower-density (higher v_A) region of the atmosphere (in $r > r_1$), and the second $(+)$ solution describes the oscillation of the higher-density (lower v_A) region ($r < r_1$). In the outer region, only a negligible twist of the magnetic field is required to maintain rigid-body behavior (i.e., $\delta B/B_r \ll \delta v/v_A$), but in the inner region, the oscillation can only be maintained by a relatively large twist (i.e., $\delta B/B_r \gg \delta v/v_A$), because of the substantial inertia of that region. If the Alfvén speed continues to decrease with decreasing r in the inner region, eventually $\omega/v'_A > 1$, and rigid-body oscillation will give way to the propagation of a torsional Alfvén wave, as is described below. In the high-frequency limit ($\omega \gg v'_A$, the WKB limit), the coupling terms on the right sides of (27) and (28) are negligible, and these equations have solutions describing inward (f) and outward (g) propagating waves:

$$f = f_0 e^{-i(\omega t + \int k\,dr)} \tag{34}$$

$$g = g_0 e^{-i(\omega t - \int k\,dr)} \tag{35}$$

$$\delta v = \left(\frac{\rho_0}{\rho}\right)^{1/4} \left[a_1 e^{-i(\omega t + \int k\,dr)} - a_2 e^{-i(\omega t - \int k\,dr)}\right] \tag{36}$$

$$\delta B = \frac{B_{r0}}{v_{A0}} \left(\frac{\rho}{\rho_0}\right)^{1/4} \left[a_1 e^{-i(\omega t + \int k\,dr)} - a_2 e^{-i(\omega t - \int k\,dr)}\right] \tag{37}$$

where a_1 and a_2 are constants. In general, of course, all the terms in (27) and (28) must be included. For the special case of an atmosphere in which the Alfvén speed varies

exponentially with height (i.e., $v_A = v_{A0} \exp[(r - r_0)/h_A]$, where h_A is a constant), (27) and (28) have the general solution (Ferraro and Plumpton, 1958)

$$\delta v = i\left(\frac{r}{r_0}\right)\left[a_3 J_0\left(\frac{\omega}{v'_A}\right) + a_4 Y_0\left(\frac{\omega}{v'_A}\right)\right] e^{-i\omega t}, \tag{38}$$

$$\delta B = -\left(\frac{r}{r_0}\right)\frac{B_r}{v_A}\left[a_3 J_1\left(\frac{\omega}{v'_A}\right) + a_4 Y_1\left(\frac{\omega}{v'_A}\right)\right] e^{-i\omega t}, \tag{39}$$

where J and Y are Bessel functions of the first and second kinds, a_3 and a_4 are constants, and $\omega/v'_A = \omega h_A/v_A$.

Using an exponentially varying Alfvén speed, one can construct a very simple model of the solar atmosphere by taking $h_A = 200$ km in $r \leq r_0$, and $h_A = \infty$ in $r > r_0$, where r_0 represents the coronal base (i.e., the top of the transition region). In such a model, we have an analytic description of the behavior of toroidal Alfvénic disturbances: δv and δB are described by (38) and (39) in the lower solar atmosphere ($r \leq r_0$) and by (36) and (37) in the corona ($r > r_0$). We can thus gain a clear understanding of all relevant physical effects, while closely reproducing the results of Hollweg (1978b), who solved numerically for δv and δB, using essentially (38) and (39), in a solar atmosphere described by 16 exponential layers. If we require that there be no inward propagating wave in $r > r_0$ (i.e., $a_1 = 0$ and $a_2 = -\delta v_0$), and that the Poynting flux and the velocity amplitude be continuous across r_0 (i.e., δv and δB are continuous across r_0), then (36)–(39) yield the real parts of δv and δB in $r < r_0$:

$$\begin{aligned}\mathrm{Re}\,\delta v = \frac{\delta v_0}{J_0 Y_1 - J_1 Y_0}\left(\frac{r}{r_0}\right)\left\{\left[Y_1 J_0\left(\frac{\omega}{v'_A}\right) - J_1 Y_0\left(\frac{\omega}{v'_A}\right)\right]\cos(-\omega t + k r_0) - \right. \\ \left. + \left[Y_0 J_0\left(\frac{\omega}{v'_A}\right) - J_0 Y_0\left(\frac{\omega}{v'_A}\right)\right]\sin(-\omega t + k r_0)\right\},\end{aligned} \tag{40}$$

$$\begin{aligned}\mathrm{Re}\,\delta B = \left(\frac{B_r}{v_A}\right)\frac{\delta v_0}{J_0 Y_1 - J_1 Y_0}\left(\frac{r}{r_0}\right)\left\{\left[Y_0 J_1\left(\frac{\omega}{v'_A}\right) - J_0 Y_1\left(\frac{\omega}{v'_A}\right)\right]\times\right. \\ \times\cos(-\omega t + k r_0) - \left[Y_1 J_1\left(\frac{\omega}{v'_A}\right) - J_1 Y_1\left(\frac{\omega}{v'_A}\right)\right]\times \\ \left.\times\sin(-\omega t + k r_0)\right\},\end{aligned} \tag{41}$$

where Bessel functions without arguments explicitly stated are evaluated at $\omega/v'_{A0} = \omega h_A/v_{A0}$, and we have set $\int k\,\mathrm{d}r = k r_0$ at r_0. As is clearly illustrated in Hollweg's (1978b) model (see his Table 1, which is based on Gingerich *et al.* (1971) and Vernazza *et al.* (1973)), the 8 order of magnitude density change from the photosphere

to the corona leads to a nearly 4 order of magnitude change in the Alfvén speed; hence, there is a broad range of frequencies over which waves can propagate in the photosphere, but cannot propagate at higher levels and are thus reflected (i.e., $\omega/v'_A \gg 1$ at the photosphere, but $\omega/v'_A < 1$ higher up). For $n = 5 \times 10^{16}\,\mathrm{cm}^{-3}$ and $B = 10\,\mathrm{G}$, $\omega/v'_A \gg 1$ if $\omega \gg 5 \times 10^{-4}\,\mathrm{s}^{-1}$, so waves with periods of several minutes or less propagate in the photosphere according to the short-wave-length (WKB) approximation. We can describe these waves by using the complex equivalents of (40) and (41) and taking the asymptotic form of the Bessel functions for large arguments ($\omega/v'_A \gg 1$):

$$\delta v = \frac{\delta v_0}{J_0 Y_1 - J_1 Y_0}\left(\frac{r}{r_0}\right)\left(\frac{v'_A}{2\pi\omega}\right)^{1/2} e^{-i(\omega t - kr_0)} \times$$

$$\times \{[(Y_1 + J_0) - i(Y_0 - J_1)]\, e^{i(\omega/v'_A - \pi/4)} +$$

$$+ [(Y_1 - J_0) - i(Y_0 + J_1)]\, e^{i(\pi/4 - \omega/v'_A)}\} \tag{42}$$

$$\delta B = \left(\frac{B_r}{v_A}\right)\frac{\delta v_0}{J_0 Y_1 - J_1 Y_0}\left(\frac{r}{r_0}\right)\left(\frac{v'_A}{2\pi\omega}\right)^{1/2} e^{-i(\omega t - kr_0)} \times$$

$$\times \{[(Y_1 + J_0) - i(Y_0 - J_1)]\, e^{i(\omega/v'_A - \pi/4)} -$$

$$- [(Y_1 - J_0) - i(Y_0 + J_1)]\, e^{i(\pi/4 - \omega/v'_A)}\}\,. \tag{43}$$

(42) and (43) clearly show that at these relatively high frequencies the Alfvénic oscillations in the photosphere are composed of outward and inward propagating waves, the latter having arisen from reflection at higher levels (but below the coronal base). The reflection coefficient (i.e., the ratio of the energy flux density in the downward propagating waves to that in the upward propagating waves) characterizing the atmosphere overlying the photosphere is thus

$$R = \frac{(Y_1 + J_0)^2 + (Y_0 - J_1)^2}{(Y_1 - J_0)^2 + (Y_0 + J_1)^2}\,. \tag{44}$$

For waves that propagate in the short-wave-length limit from the photosphere to the top of the transition region, there is virtually no reflection:

$$R \approx 0 \qquad (\omega \gg v'_{A0})\,. \tag{45}$$

For a wave that must 'tunnel through' to the corona because its wavelength becomes greater than the local scale-hieght well before the corona is reached, most of the energy is reflected:

$$R \approx 1 - 2\pi\omega h_A / v_{A0} \qquad (\omega \ll v'_{A0}) \tag{46}$$

and a standing wave is produced in the lower solar atmosphere, as pointed out by Hollweg (1978b). Hollweg (1972, 1978b, 1982) claims that the standing wave pattern is caused by reflections at discontinuities in the density scale height. In fact, coupling

between inward and outward propagating waves is an integrated effect, and a finite jump in the refractive index is required to produce an inward propagating wave of finite amplitude (cf. Alfvén and Fälthammar, 1963; Heinemann and Olbert, 1980). We must agree, therefore, with the interpretation of Ferraro and Plumpton (1958): viz., that the Alfvén waves are reflected due to the continuous variation of the refractive index. The features of such a standing wave pattern are readily determined using (40) and (41), and one example, for $\omega/v'_{A0} = 10^{-3}$, is shown in Figure 6.

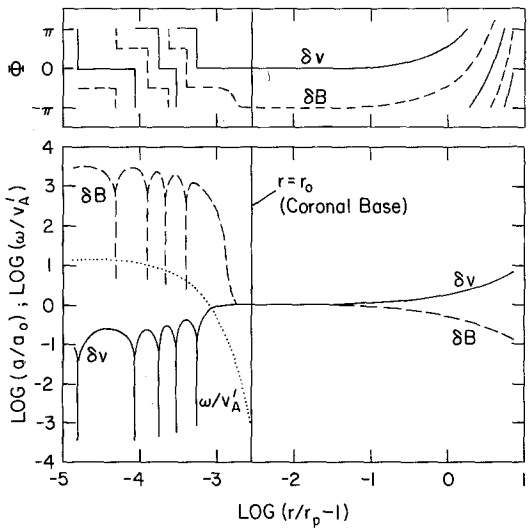

Fig. 6. Amplitudes (a_v and a_B) and phases (Φ_v and Φ_B) of δv and δB, and the dimensionless ratio ω/v'_A plotted as functions of height above the photosphere ($r/r_p - 1$). The amplitudes and phases are defined by $\delta v = a_v \cos(-\omega t + \Phi_v)$ and $\delta B = a_B \cos(-\omega t + \Phi_B)$, where $a_{v0} = \delta v_0$ and $a_{B0} = \delta B_0$. Below the coronal base ($r \leq r_0$) the Alfvén speed scale-height, h_A, is 200 km, and above the coronal base ($r > r_0$)$h_A = \infty$. For $\log(r/r_p - 1) > 1$, the a_v and a_B curves approach straight lines. Regions of standing waves ($\log(r/r_p - 1) \lesssim -2.8$), rigid-body oscillation ($-2.75 \lesssim \log(r/r_p - 1) < -2.55$), and outward propagating waves ($\log(r/r_p - 1) > -2.55$, corresponding to $r > r_0$) can be seen.

In Figure 6 we see that the toroidal Alfvénic disturbances propagate outward as simple waves above the coronal base ($r > r_0$), give rise to rigid-body oscillation of the atmosphere just below the coronal base, and produce a standing wave pattern in the lower atmosphere. The minima in the standing wave pattern are imperfect nodes (i.e., δv, $\delta B \neq 0$ at the nodes). The reflection caused by the Alfvén-speed gradient is very efficient at this frequency $\omega = 10^{-3}\, v'_{A0}$: reference to (46) indicates that only 0.6% of the energy carried by upward propagating waves in the photosphere reaches the corona; the rest is reflected. It has been noted (Hollweg, 1978b) that if the generation of the Alfvén waves takes place at some particular location near the top of the convection zone, then at certain 'resonant' frequencies a node will be located at the generation point, and a modest velocity perturbation (δv) will correspond to a very large magnetic perturbation (δB) and thus to a very large energy flux at that frequency. Of course, to produce such a large energy flux by driving the wave at a node there are three necessary requirements:

(1) the wave driver must be phase-coherent over many wave periods; (2) the wave generation region must be narrow in height and remain at a fixed height over many wave periods; (3) the frequency for which the preceding two conditions are met must correspond to the presence of a node in the wave generation region. It seems unlikely that these three requirements, or their equivalent, will be met in the real solar atmosphere, and we conclude that the large 'resonant' energy fluxes discussed by Hollweg (1978b) are an artefact of the model considered and should not be invoked in discussing the transport of energy from the photosphere to the corona.

On the basis of the preceding analysis and of the observational results presented by Athay and White (1979b), we can place limits on the energy flux that can be transported from the lower solar atmosphere to the corona by Alfvén waves. At the atmospheric levels where observational information on δv is available, if $\omega \gg v'_A$ the energy flux density passing into the corona is given by

$$\phi_A = nm \langle \delta v^2 \rangle v_A (1 - R), \tag{47}$$

where R is given by (46). Even if $\omega > v'_{A0}/2\pi$, (47) is approximately correct provided we take $R = 0$ (cf. (45)). If $\omega \ll v'_A$ there is rigid body oscillation everywhere above the level where δv is measured, so $\delta v_0 \approx \delta v$ and

$$\phi_A \approx n_0 m < \delta v^2 > v_{A0} . \tag{48}$$

When ω is comparable to v'_A (47) and (48) can be used in conjunction to estimate ϕ_A. Applying the above procedure to the data provided in Table 1 of Athay and White (1979b) leads us to conclude that Alfvén waves generated in the upper chromosphere or below, with wave periods between about 30 and 3000 s, can provide an energy flux density of no more than 1×10^5 erg cm^{-2} s^{-1} to the corona. For wave periods of longer than one hour, a large-scale Alfvén wave might give rise to a Doppler shift of spectral lines rather than simply to line broadening, which is the effect on which the preceding interpretation is based. For such long periods, however, the atmosphere will be in rigid body motion everywhere from the middle chromosphere to the corona, so that an energy flux entering the corona of more than 10^5 erg cm^{-2} s^{-1} at these periods would correspond to chromospheric velocities of more than 10 km s^{-1}. As such large chromospheric Doppler shifts are not observed, the upper limit given above would seem to apply to these longer periods as well. Finally, one might expect that very short period waves ($\tau \lesssim$ a few seconds) could carry larger energy fluxes to the corona, given the observational constraints on the velocity amplitude in the lower solar atmosphere, but these waves tend to be damped strongly by viscous and frictional effects in the photosphere and the chromosphere (Osterbrock, 1961). Of course, energy flux densities of the order 10^5 erg cm^{-2} s^{-1} in the corona generally imply non-linear waves in the photosphere and lower chromosphere, and such waves should be strongly damped in these lower regions (Parker, 1960; Osterbrock, 1961). We conclude, therefore that an energy flux density of more than 10^5 erg cm^{-2} s^{-1} carried into the region of supersonic solar wind flow by Alfvén waves cannot have been transported upward from the photosphere or chromosphere by Alfvén waves alone and thus must have arisen, at least

in part, from the generation of Alfvén waves in the transition region or the lower corona.

In the simple model described above, with $h_A = \infty$ above the coronal base, Alfvén waves of all frequencies propagate as short-wave-length (WKB) waves in the corona and the solar wind. In reality, of course, v_A does vary above the coronal base, and waves with periods longer than a few hours do not propagate so simply in this region. The description of non-WKB effects becomes a bit more complicated in this case, however, because one can no longer assume that $u \ll v_A$, and (27) and (28) must be replaced (Heinemann and Olbert, 1980) by

$$\left[\frac{\partial}{\partial t} + (u - v_A)\frac{\partial}{\partial s}\right] f = \tfrac{1}{2} g(u - v_A)\frac{\mathrm{d} \ln v_A}{\mathrm{d}r}, \tag{49}$$

$$\left[\frac{\partial}{\partial t} + (u + v_A)\frac{\partial}{\partial s}\right] g = \tfrac{1}{2} f(u + v_A)\frac{\mathrm{d} \ln v_A}{\mathrm{d}r}, \tag{50}$$

where $\mathrm{d}s$ is a length element along the magnetic field ($\mathbf{u} \times \mathbf{B} = 0$), which is no longer assumed radial, and f and g are related to δv and δB through

$$\delta v = \tfrac{1}{2}\eta^{1/4}\left(\frac{f}{1 - \eta^{1/2}} + \frac{g}{1 + \eta^{1/2}}\right), \tag{51}$$

$$\delta B = \frac{B}{v_A}\,\tfrac{1}{2}\eta^{1/4}\left(\frac{f}{1 - \eta^{1/2}} - \frac{g}{1 + \eta^{1/2}}\right), \tag{52}$$

where $\eta = \rho/\rho_a$, and the subscript a refers to the Alfvén point, where $u = v_A$. Well inside the Alfvén point, $u \ll v_A$, and the discussion of simple wave propagation and rigid body oscillation in connection with (27) and (28) applies quite well, but when $u \gtrsim v_A$ the problem is more complicated, and numerical solutions to (49) and (50) are generally required (cf. Figure 7). There is, however, a simple case of some interest in which analytic solutions to these equations exist: i.e., the case in which $\omega \to 0$ ($\partial/\partial t$ terms negligible) for a toroidal Alfvénic disturbance that is symmetric about the solar rotation axis. This is, of course, the case considered by Weber and Davis (1967), in which the Alfvénic disturbance of zero frequency corresponds to solar rotation; the solutions to (49) and (50) are (Heinemann and Olbert, 1980)

$$f \propto \left[\left(\frac{v_A}{v_{Aa}}\right)^{1/2} - \left(\frac{v_{Aa}}{v_A}\right)^{1/2}\right] e^{-i\omega t}, \tag{53}$$

$$g \propto \left[\left(\frac{v_A}{v_{Aa}}\right)^{1/2} + \left(\frac{v_{Aa}}{v_A}\right)^{1/2}\right] e^{-i\omega t}, \tag{54}$$

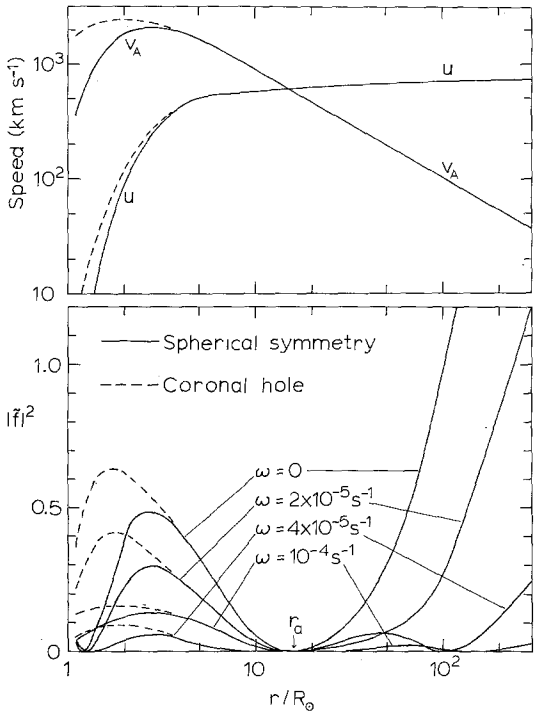

Fig. 7. The background flow speed and Alfvén speed as functions of radial distance for a spherically symmetric flow geometry (solid lines) and for the average rapidly diverging flow geometry implied by the coronal hole boundary of Munro and Jackson (1977) (dashed lines). The inward-propagating wave amplitudes, $|\tilde{f}|^2$, for different wave frequencies ω, are shown as functions of radial distance for the spherical and rapidly diverging flow geometries (adapted from Heinemann and Olbert (1980)).

and these give velocities and magnetic fields agreeing with those of Weber and Davis (1967). In obtaining (53) and (54), the boundary condition $f_a = 0$ is applied. That this is always a sensible condition is readily seen by considering the facts that f and g correspond to inward and outward propagating waves (though f and g are not proper eigenmodes of the system) and that in $r > r_a$ the inward wave (f) is convected outward by the super-Alfvénic flow.

If we define $\tilde{f} = f e^{i\omega t}$ and $\tilde{g} = g e^{i\omega t}$ and normalize such that $|\tilde{g}|^2 - \tilde{f}^2 = 1$, then the condition $|\tilde{f}_a|^2 = 0$ (and thus $|\tilde{g}_a|^2 = 1$) leads to the results (Heinemann and Olbert, 1980) shown in Figure 7 for toroidal Alfvénic disturbances in a spherically symmetric and a rapidly expanding coronal expansion. When the coupling between outward and inward propagating waves is weak, $|\tilde{f}|^2 \ll |\tilde{g}|^2$, and the disturbance propagates outward as a simple (WKB) wave. Inside the Alfvén radius (i.e., in $r < r_a$), the coupling is very weak for wave periods of a few hours or less, but is significant for periods of a day or longer. Coronal hole geometries, which lead to a decrease in the scale length over which v_A varies, cause only slightly stronger coupling (near the coronal base) than is found for spherical geometry. Outside the Alfvén radius (i.e., in $r > r_a$), the coupling again is very weak for periods of a few hours or less, but strong for periods of more than a day. In all regions the maximum coupling is attained as $\omega \to 0$ and

$|\tilde{f}|^2 \to \frac{1}{4}(v_A/v_{Aa} + v_{Aa}/v_A) - \frac{1}{2}$. (For a more detailed discussion of these points, see Heinemann and Olbert (1980).)

The force exerted by the Alfvénic oscillations on the solar wind plasma is composed of a centrifugal force and a Lorentz force (the centrifugal force being important only when the coupling is strong). This force varies on a time scale $\tau/4$, where $\tau = 2\pi/\omega$ is the wave period, and this time scale can be compared with the solar wind expansion time, $\tau_{exp} = |(u/n)(dn/dr)|^{-1}$. If $\tau \ll \tau_{exp}$ the solar wind responds to the average effect of the force over a wave period, but if $\tau \gtrsim \tau_{exp}$ the variation of the force over a wave period must be considered. In the following section we shall assume that $\tau \ll \tau_{exp}$, although for waves with $\tau \gtrsim 1$ hour this assumption will break down, most severely in the vicinity of the sonic point, where τ_{exp} is smallest.

5. Interaction of Alfvén Waves with the Solar Wind

A simple illustration of energy addition to the solar wind is provided by the interaction of Alfvén waves with the solar wind. The simplicity arises, in part, from the fact that Alfvén waves transport energy along the magnetic field, which allows us to continue to describe solar wind flow along an isolated infinitesimal flow tube. Because linear damping of these waves is very weak above the coronal base, their energy is not dissipated as heat in the plasma until the wave amplitude becomes very large (i.e., $\delta B \approx B$), and for reasonable wave energy fluxes this does not occur in the region of subsonic flow. Consequently, Alfvén waves, through the force associated with the gradient in their energy density, supply only momentum (not heat) to the subsonic solar wind. In the supersonic region, both heat and momentum are added, as non-linear dissipation becomes important. This energy addition by Alfvén waves, then, affects both the solar wind mass flux and energy flux, and determination of its effect on the solar wind flow speed at 1 AU requires careful consideration.

The subject of Alfvén waves in the solar wind has been considered by several workers (e.g., Alazraki and Couturier, 1971; Belcher, 1971; Hollweg, 1973, 1978a; Jacques, 1977; see also references given by Hollweg, 1978a). These authors have all made use of the short-wave-length (WKB) approximation, as shall we in the following discussion (cf. Section 4 and Heinemann and Olbert, 1980). In general, little attention has been given to the coronal base boundary conditions: frequently, the base density has been allowed to take on unrealistically low values so as to produce a reasonable solar wind mass flux. We shall reproduce here the essential results of the several studies mentioned above, but we shall fix the coronal base pressure at a realistic value and investigate the effects of Alfvén waves on the mass flux, energy flux, and flow speed at 1 AU, in a manner similar to that employed in discussing the general subject of energy addition in Section 3. Our approach will involve simplifying the model of Hollweg (1978a), so that it retains the basic physics but admits analytic solutions, which should provide us with greater physical insight into the problem (cf. Leer *et al.*, 1980).

Let us begin by reconsidering the conservation laws used to describe energy addition in the solar wind. The mass conservation Equation (1) remains unchanged, and the

momentum Equation (13) is specialized by associating the force per unit mass, D, with the Alfvén wave pressure gradient:

$$D = -\frac{1}{\rho}\frac{\mathrm{d}}{\mathrm{d}r}\left(\frac{\langle \delta B^2 \rangle}{8\pi}\right). \tag{55}$$

We replace the energy Equation (15) by the assumption that the temperature is constant in the subsonic region ($T = T_0$ in $r_0 \leq r \leq r_c$) and that the solar wind energy flux at the critical point is given by

$$F_c = \mathscr{F}\left[\tfrac{1}{2}u_c^2 + (5 + \tfrac{3}{2}\alpha)\frac{kT_0}{m} - \frac{GM}{r_c}\right]. \tag{56}$$

This treatment of energy balance produces results very similar to those that are obtained using Hollweg's (1976) description of thermal conduction (cf. Sections 2 and 3 and Hollweg, 1978a), but allows us to derive an analytic description and thus to illuminate, in a simple way, the important physical effects of Alfvén waves on the solar wind.

The force on the solar wind due to Alfvén waves, given in (55), can be expressed in terms of coronal base parameters and the solar wind density by employing the principle of conservation of wave action (e.g., Dewar, 1970; Bretherton, 1970; Jacques, 1977), which allows us to write the Alfvén-wave energy density, ε, and energy flux, F_W, as follows:

$$\varepsilon = \frac{\langle \delta B^2 \rangle}{4\pi} = \varepsilon_0 \frac{M_{A0}}{M_A}\left(\frac{1 + M_{A0}}{1 + M_A}\right)^2 \tag{57}$$

$$F_W = F_{W0}\frac{1 + \frac{3}{2}M_A}{1 + \frac{3}{2}M_{A0}}\left(\frac{1 + M_{A0}}{1 + M_A}\right)^2 \tag{58}$$

where $M_A = u/v_A$ and $F_W = \varepsilon(v_A + \frac{3}{2}u)A$. Now we can write the equation of motion describing the solar wind expansion in the presence of Alfvén waves in a standard form:

$$\frac{1}{u}\frac{\mathrm{d}u}{\mathrm{d}r}\left(u^2 - \frac{2kT^*}{m}\right) = \frac{2kT^*}{m}\frac{1}{A}\frac{\mathrm{d}A}{\mathrm{d}r} - \frac{GM}{r^2}, \tag{59}$$

where we have defined the effective temperature, T^*, by

$$\frac{2kT^*}{m} = \frac{2kT_0}{m} + \frac{1}{4}\left(\frac{1 + 3M_A}{1 + M_A}\right)\langle \delta v^2 \rangle, \tag{60}$$

and in the WKB limit $\langle \delta v^2 \rangle = \langle \delta B^2 \rangle / 4\pi\rho$. (59) has the same form as the equation of motion describing a solar wind expansion driven only by the thermal pressure, with

$p = 2nkT^*$; indeed, $(2kT^*/m)^{1/2}$ measures the speed at which a compressive wave propagates parallel to the magnetic field in the subsonic solar wind plasma in the presence of relatively short-wave-length Alfvén waves. Thus the critical point at $r = r_c$, where

$$r_c = \frac{GMm}{4kT_c^*\beta_c}, \tag{61}$$

$$u_c = (2kT_c^*/m)^{1/2}, \tag{62}$$

is appropriately considered the point separating subsonic from supersonic flow. To understand why the presence of Alfvén waves modifies the speed with which a compressive wave propagates, we must remember that the Alfvén-wave energy density depends on the plasma density (cf. (57));

$$\langle \delta B^2 \rangle \propto \rho^{1/2}\zeta(\rho), \tag{63}$$

where $\zeta(\rho) = [(1 + M_{A0})/(1 + M_A)]^2 \approx 1$ for $M_A \ll 1$. When the plasma is compressed, therefore, both the internal energy density of the plasma ($\propto \rho T$) and the Alfvén-wave energy density ($\propto \langle \delta B^2 \rangle$) are increased, and the restoring force in a compressive wave, which depends on the gradient of the total perturbed energy density, is larger than it would be in the absence of Alfvén waves.

We are now in a position to calculate the effect of Alfvén waves on the solar wind mass flux, energy flux, and flow speed at 1 AU. Making use of definitions of f and β in Section 2, we can integrate (59) from the coronal base ($r = r_0$) to the critical point ($r = r_c$) to obtain the solar wind proton flux density at 1 AU:

$$n_E u_E = n_0(v_T^2 + \tfrac{1}{4}\langle \delta v_c^2 \rangle)^{1/2} \times \\ \times \left(\frac{f_c r_c^2}{f_E r_E^2}\right) \exp\left[-\frac{v_{e0}^2}{2v_T^2} + (2\beta_c + \tfrac{3}{2})\frac{\delta v_c^2}{4v_T^2} + (2\beta_c - \tfrac{1}{2}) \right], \tag{64}$$

where $v_e^2 = 2GM/r, v_T^2 = (2kT/m)^{1/2}$, and we have assumed $u_0^2 \ll 2kT_0/m, (n_c/n_0)^{1/2} \ll 1$, and $M_{A0} < M_{AC} \ll 1$. When $\delta v_c \to 0$, (64) reduces to (8), as it should. (64) indicates that the presence of Alfvén waves in the solar wind tends to increase the mass flux, as was anticipated in the discussion of momentum addition in Section 3. The mass flux ($\propto n_E u_E$) can be expressed in terms of coronal base parameters (except for f_c and β_c) if we can relate δv_c to δv_0. From (57) we find $\langle \delta v_0^2 \rangle = \langle \delta v_c^2 \rangle (n_c/n_0)^{1/2}$ and use of (64) enables us to obtain an implicit equation expressing the desired relation:

$$\langle \delta v_0^2 \rangle^2 = \langle \delta v_c^2 \rangle^2 \exp\left[-\frac{v_{e0}^2}{2v_T^2} + (2\beta_c + \tfrac{3}{2})\frac{\langle \delta v_c^2 \rangle}{4v_T^2} + (2\beta_c - \tfrac{1}{2}) \right]. \tag{65}$$

Since virtually all the solar wind energy flux is carried by the flow at 1 AU in a model like the one we are using, the flow speed at 1 AU is given by

$$\tfrac{1}{2}u_E^2 = (F_c + F_{Wc})/\mathcal{F}, \tag{66}$$

where $\mathcal{F} = n_E m u_E f_E r_E^2$ is given by (64), F_c by (56), and F_{Wc} by (58). (64)–(66) allow

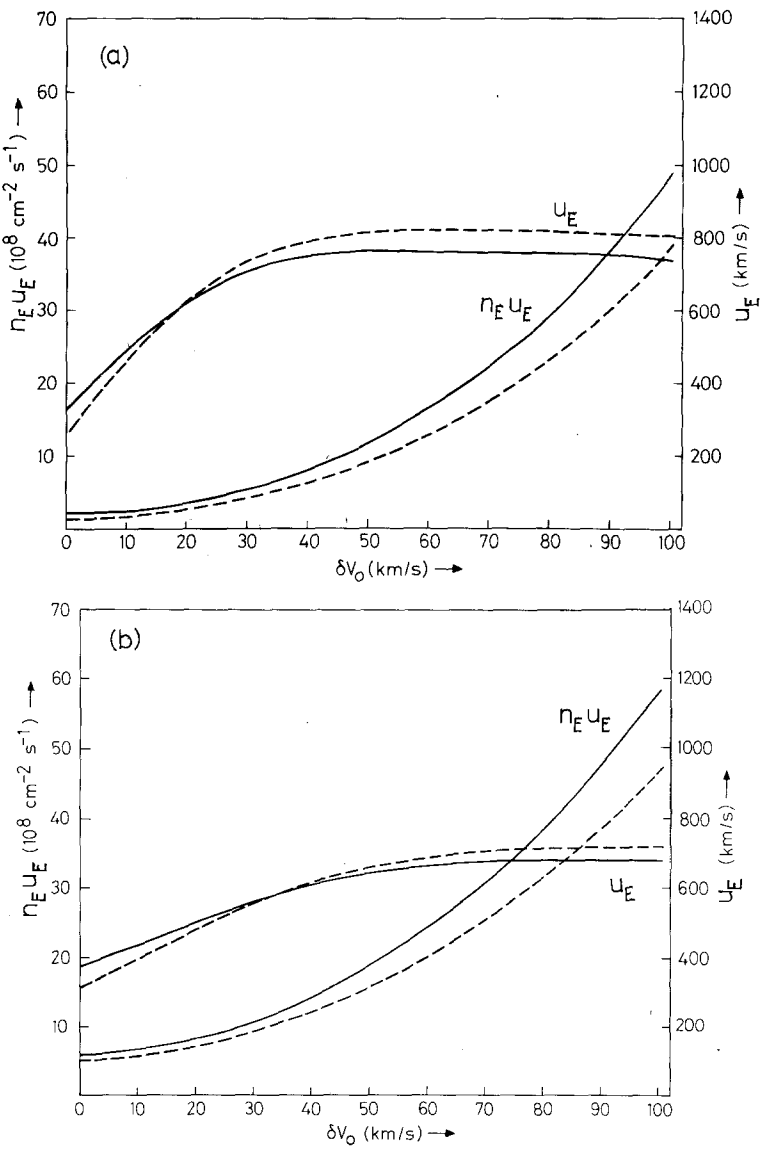

Fig. 8. Proton flux density ($n_E u_E$) and flow speed (u_E) at 1 AU as functions of the coronal-base Alfvén-wave amplitude ($\delta v_0 = \sqrt{\langle \delta v_0^2 \rangle}$). The coronal-base pressure is specified by $n_0 T_0 = 2 \times 10^{14}$ cm^{-3} K, the (radial) magnetic field at 1 AU is $B_E = 4 \times 10^{-5}$ G, and the coronal temperature is $T_0 = 1.1 \times 10^6$ K in (a) and $T_0 = 1.3 \times 10^6$ K in (b). Results for both spherically symmetric flow (solid curves) and rapidly expanding flow (dashed curves), with $f_E = 7$, $f_c = 5$, and $\beta_c = 1.5$, are shown.

us to calculate u_E and $n_E u_E$ in terms of coronal base parameters, and some results of such calculations are shown in Figures 8, 9, and 10.

Figure 8 illustrates the effects of varying the Alfvén-wave velocity amplitude at the coronal base (δv_0) on the solar wind mass flux ($\propto n_E u_E$) and flow speed (u_E). When the wave energy density is small in comparison with the thermal energy density (i.e., $\langle \delta v_0^2 \rangle \ll v_T^2$) the mass flux is determined primarily by the temperature, and varying δv_0 affects $n_E u_E$ very little. For a sufficiently large magnetic field, however, the energy flux carried by the waves ($\propto B_0 \langle \delta v_0^2 \rangle \rho_0^{1/2}$) can be large enough that increasing δv_0 can substantially increase u_E when $n_E u_E$ is essentially unchanged (cf. (66)). This behavior is illustrated in Figure 8 for $\delta v_0 \lesssim 30$ km s^{-1}. For larger δv_0, the Alfvén waves begin to play a significant role in determining the mass flux, leading to such a rapid increase in $n_E u_E$ with increasing δv_0 that u_E peaks and actually begins to decrease slowly as δv_0 continues to increase (cf. (66)). For higher coronal temperature ($T_0 = 1.1 \times 10^8$ K in Figure 8a and $T_0 = 1.3 \times 10^8$ K in Figure 8b), the change in u_E produced by a given

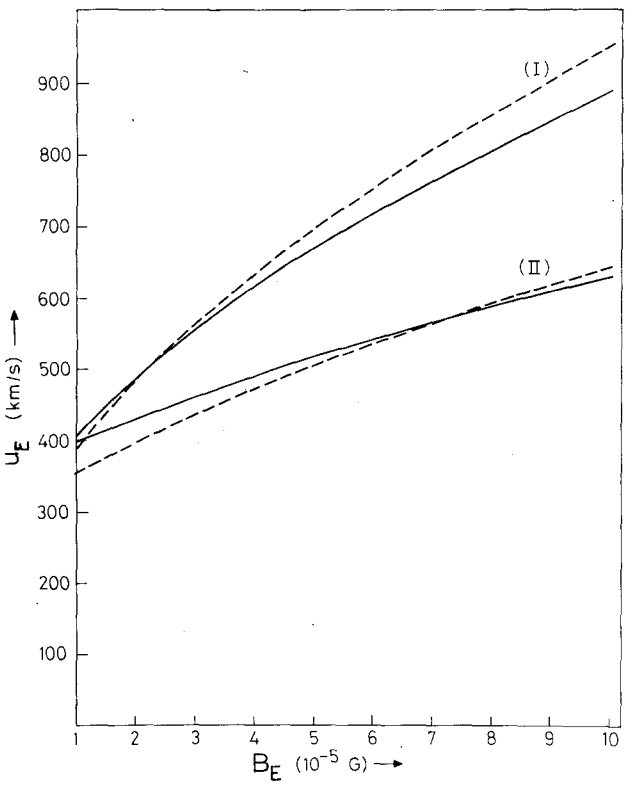

Fig. 9. Flow speed at 1 AU (u_E) as a function of magnetic field strength at 1 AU (B_E), for $\delta v_0 = 20$ km s^{-1}, $T_0 = 1.1 \times 10^6$ K (I) and 1.3×10^6 K (II), and otherwise the same parameters as Figure 8. The particle flux densities at 1 AU are $n_E u_E = 3.5 \times 10^8$ cm^{-2} s^{-1} (I) and 8.3×10^8 cm^{-2} s^{-1} (II) for spherical symmetry (solid curves) and 2.9×10^8 cm^{-2} s^{-1} (I) and 7.0×10^8 cm^{-2} s^{-1} (II) for rapidly expanding flow (dashed curves).

Alfvén wave energy flux ($\propto B_0 \langle \delta v_0^2 \rangle \rho_0^{1/2}$) is not as large, because the mass flux is larger for the higher temperature and the energy per unit mass supplied by the Alfvén waves is correspondingly lower. Note that rapidly expanding flow geometries (dashed curves) do not lead to results significantly different from those for spherically symmetric flow.

The importance of the magnitude of the magnetic field is illustrated in Figure 9, where δv_0 ($= 20$ km s^{-1}) is held constant. Because the mass flux depends on $\langle \delta v_0^2 \rangle$, not B_0, whereas the energy flux depends on both, only u_E is plotted as a function of B_0 (note: $B_0 = B_E f_E r_E^2 / r_0^2$). The monotonic increase of the Alfvén-wave energy flux with increasing B_0 gives rise to the increase in u_E with increasing $B_E (\propto B_0)$, and the higher flow speeds associated with lower coronal temperature reflect the effect of the lower mass flux arising from lower T_0 (cf. (64), (66)). Figure 10 shows several of the requirements

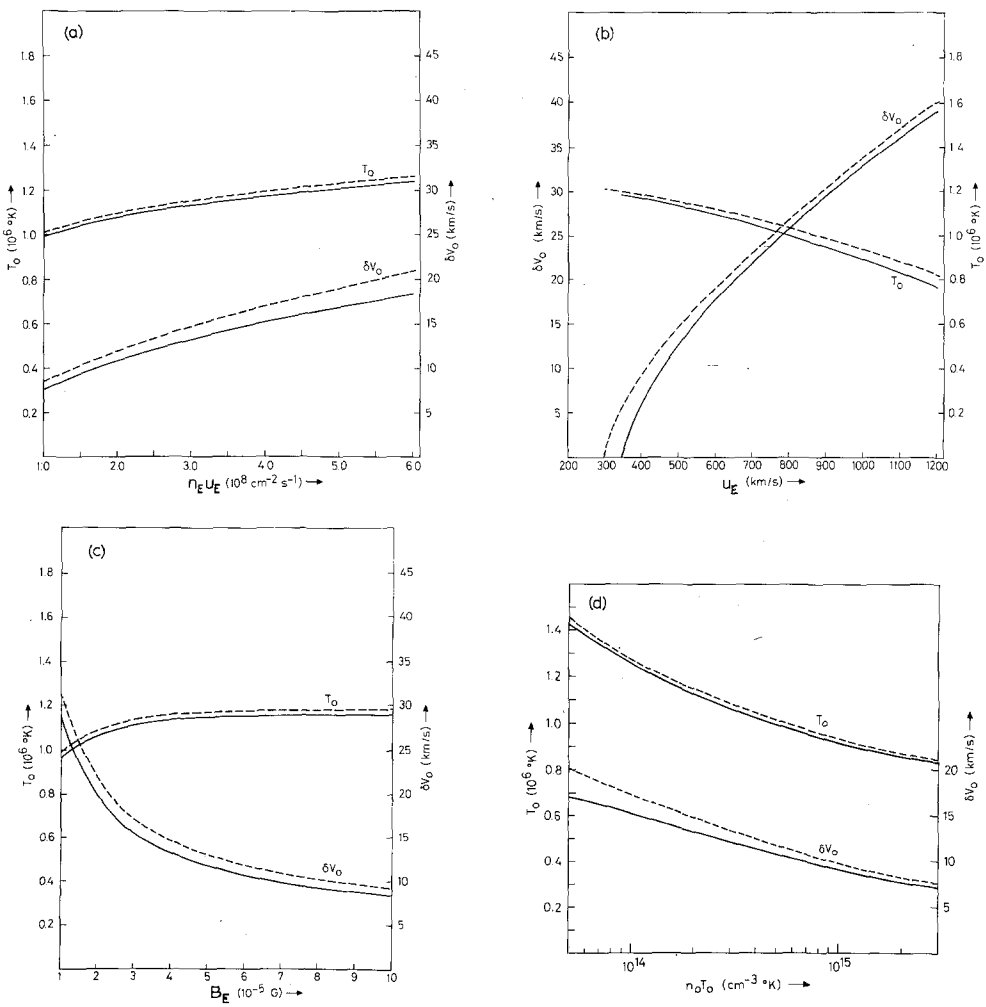

Fig. 10. Parameter variations for the basic model used in Figures 8 and 9, with the additional reference parameters of $B_E = 4 \times 10^{-5}$ G in (a), (b), and (d), $u_E = 500$ km s^{-1} in (a), (c), and (d), and $n_E u_E = 3 \times 10^8$ cm^{-2} s^{-1} in (b), (c), and (d).

on coronal parameters if Alfvén waves are to play a role in driving high-speed solar wind streams, given observational constraints on $n_E u_E$, u_E, and $n_0 T_0$: (b) larger wave amplitudes and lower coronal temperatures lead to higher-speed winds ($n_E u_E$ and $n_0 T_0$ fixed); (a) a narrow range of values of T_0 and δv_0 are possible if a high-speed stream is to have a reasonable mass flux; (d) even a broad range of observationally acceptable values of the coronal base pressure (say, $10^{14} \lesssim n_0 T_0 \lesssim 6 \times 10^{14}$ cm^{-3} K) provide little latitude for variations of δv_0 and T_0; (c) the same is true for acceptable values of $B_0 (= B_E f_E r_E^2 / r_0^2)$.

From the preceding results, one can see that it is not unreasonable to suppose that high-speed streams can be produced in a solar wind with Alfvén waves present, if $\delta v_0 \approx 20$–30 km s^{-1}. Yet the observational constraints at 1 AU of $n_E u_E \approx 3 \times 10^8$ cm^{-2} s^{-1} and $2 \times 10^{-5} \lesssim B_E \lesssim 7 \times 10^{-5}$ G (e.g., Feldman *et al.*, 1977) and at the coronal base of $10^{14} \lesssim n_0 T_0 \lesssim 6 \times 10^{14}$ cm^{-3} s^{-1} (e.g. Withbroe, 1977) place such tight restrictions on possible values of δv_0 and T_0 that one must be very careful in drawing any definitive conclusions. At present, we can only say that the high-speed stream models invoking Alfvén waves as a source of additional energy can be made consistent with the limited coronal observations available (see Withbroe (1982) for inferences regarding δv_0 and T_0).

6. Stellar Winds Driven by Alfvén Waves

Late-type giant and supergiant stars frequently exhibit cool, massive stellar winds (see reviews by Cassinelli (1979) and Cassinelli and MacGregor (1982) and references therein), and it has been suggested that Alfvén waves might play an important role in driving such winds (Belcher and Olbert, 1975; Hartmann and MacGregor, 1980; Holzer *et al.*, 1982). Because the models proposed to describe these stellar winds differ in important respects from that for the solar wind, discussed in Section 5, it will be instructive to consider briefly a representative stellar wind model. In such a model (e.g. Hartmann and MacGregor, 1980), the temperature of the atmosphere ($\approx 10^4$ K) is so low that the thermal pressure gradient force is relatively unimportant, but the stellar gravity is so weak ($M_* R_\odot^2 / M_\odot R_*^2 \approx 10^{-4}$) that a moderate Alfvén-wave energy flux density ($\approx 10^6$ erg cm^{-2} s^{-1} at the stellar surface) can drive a quite massive wind. The winds, however, are so cool and dense that frictional damping of the Alfvén waves (cf. Section 4 and Osterbrock, 1961) and radiative energy loss from the plasma play important roles. We can understand most of the relevant physical effects in such models by taking a simple approach, similar to that of Section 5.

Let us consider a one-fluid, isothermal model: mass conservation is given by (1), momentum conservation by (13) and (55), and energy conservation by $T = T_0 =$ constant, in place of (14) or (15). The isothermal assumption is a reasonable first approximation, because energy balance in such an atmosphere consists basically of a balance between wave heating and radiative cooling, and the latter depends so strongly on temperature that the variation of temperature through the region of subsonic flow is generally quite modest, even if the wave-heating rate varies considerably. An

important implication of this energy balance is that a substantial fraction of the Alfvén-wave energy flux can be lost to the stellar radiation field, whereas in the solar case virtually the entire wave flux is converted into the flow energy of the wind.

If the local damping length of the Alfvén waves is L, then (57) and (58) are modified by the same exponential factor: viz., (57) becomes

$$\varepsilon = \frac{\langle \delta B^2 \rangle}{4\pi} = \varepsilon_0 \frac{M_{A0}}{M_A}\left(\frac{1 + M_{A0}}{1 + M_A}\right)^2 \exp\left(-\int_{r_0}^{r} dr' L^{-1}\right), \tag{67}$$

where the subscript 0 refers to the reference level $r = r_0$. Combining (1), (3), (13), (55), and (67), the stellar wind equation of motion for spherical symmetry is obtained:

$$\frac{1}{u}\frac{du}{dr}\left[u^2 - v_T^2 - \frac{1}{4}\left(\frac{1 + 3M_A}{1 + M_A}\right)\langle \delta v^2 \rangle\right] =$$

$$= \frac{2}{r}\left[v_T^2 + \frac{1}{4}\left(\frac{1 + 3M_A}{1 + M_A}\right)\langle \delta v^2 \rangle + \frac{1}{4}\frac{r}{L}\langle \delta v^2 \rangle - \frac{1}{4} v_e^2\right]. \tag{68}$$

(Note that (68) differs from (59) only in the damping term, $(r/4L)\langle \delta v^2 \rangle$.) Before discussing solutions of (68), let us consider the limit of weak damping ($L \to \infty$), low temperature ($v_T^2 \ll \langle \delta v^2 \rangle$), strong radial magnetic field ($M_{AC} \ll 1$), and moderate wave amplitude ($\delta v_0^2 \ll v_{e0}^2$). It is then readily shown that

$$r_c = 1.75 r_0\,, \tag{69}$$

$$\rho_c = \rho_0 (1.75 \langle \delta v_0^2 \rangle / v_{e0}^2)^2\,, \tag{70}$$

$$\rho_0 u_0 = \tfrac{1}{2}(1.75)^{7/2} \rho_0 v_{e0}^{-3} \langle \delta v_0^2 \rangle^2\,. \tag{71}$$

If we take r_0 to be the stellar radius, B_* to be the stellar surface magnetic field in Gauss, and f_{w*} to be the Alfvén wave energy flux density in units of 10^6 erg cm^{-2} s^{-1} at $r = r_0$, and if we define $R_* = r_0/R_\odot$ and $M_* = M/M_\odot$, the mass loss rate driven by Alfvén waves, in units of solar masses per year, is

$$-\dot{M} = 1.8 \times 10^{-13}\left(\frac{f_{w*} R_*}{B_*}\right)^2 \left(\frac{R_*}{M_*}\right)^{3/2}. \tag{72}$$

If all the Alfvén wave energy flux is eventually converted into flow energy, the asymptotic flow speed, u_∞, can be calculated from the energy conservation requirement that $u^2 - v_e^2 + 2\langle \delta v^2 \rangle / M_A = \text{const}$:

$$u_\infty^2 = v_{e0}^2\left[2.8 \frac{B_*^2}{f_{w*}}\left(\frac{M_*}{R_*}\right)^{1/2} - 1\right] \tag{73a}$$

$$= v_{e0}^2\left(\frac{8}{7M_{AC}} - \frac{3}{7}\right). \tag{73b}$$

For $R_* \gg M_* \gg 1$, as is the case for the cool giants and supergiants under consideration, (72) indicates that undamped Alfvén waves can drive a quite massive wind, when their energy flux density is of the order 10^6 erg cm^{-2} s^{-1} and the stellar magnetic field is a few Gauss or less. If the requirement $M_{AC} \ll 1$ (which is necessary for (69)–(73) to be valid) is met, then (73b) indicates that the asymptotic flow speed is much larger than the gravitational escape speed at the stellar surface. As we shall see, this large asymptotic flow speed seems to raise difficulties for the models of Alfvén-wave-driven stellar winds.

The problem we encountered in the solar wind (cf. Section 2, 3, and 5) was to explain the relatively low mass flux and high asymptotic flow speed. For winds from cool giants and supergiants the problem is just the reverse: it is necessary to explain very large mass fluxes and very low asymptotic flow speeds (i.e., $u_\infty^2 \ll v_{e0}^2$). (73b) illustrates the difficulty one encounters in trying to drive such winds with undamped Alfvén waves: viz., too high an asymptotic flow speed is produced. As we shall see later, this difficulty continues to plague us even when the effects of wave damping are included. Before discussing damping, however, let us consider the transition from thermally dominated winds (cf. Sections 2 and 5) to wave dominated winds (cf. (69)–(73)), in the context of undamped Alfvén waves.

For this purpose, we can use (56) and (64)–(66), for which it was assumed that $M_{A0} < M_{AC} \ll 1$, $u_0^2 \ll 2kT_0/m$, and $(n_c/n_0)^{1/2} \ll 1$. We can readily eliminate the latter two assumptions and include the generally small terms that become important as $r_c \to r_0$. Solutions to these equations are shown in Figure 11. In a thermally dominated wind, the critical point is seen to move inward with increasing temperature, eventually reaching the coronal base (cf. Figure 11a in the region $v_T^2/v_{e0}^2 > 5 \times 10^{-2}$ and (61) in the limit $\langle \delta v^2 \rangle \to 0$). As the temperature decreases, however, a maximum critical point radius is reached (near $v_T^2/v_{e0}^2 = 5 \times 10^{-2}$ for $10^{-4} \lesssim \langle \delta v_0^2 \rangle / v_{e0}^2 \lesssim 10^{-2}$), and as the temperature continues to decrease the critical point moves inward, approaching $r_c = 1.75 r_0$, as long as $\delta v_0^2/v_{e0}^2 \lesssim 10^{-2}$ (cf. (69)). This behavior of the critical point is an indication of the transition to the dominance of wave effects over the thermal effects, and this transition to wave-dominance occurs when $\langle \delta v_0^2 \rangle \ll v_T^2$, because $\langle \delta v^2 \rangle (\propto \rho^{-1/2})$ increases rapidly with radial distance as the density scale-height decreases (cf. (65)). In the limit $v_T^2/v_{e0}^2 \to 0$, the Alfvén waves completely control the radial atmospheric structure, and the density scale-height is determined by $\langle \delta v_0^2 \rangle / v_{e0}^2$ (cf. (70)). As the velocity amplitude of the waves becomes large ($0.1 \lesssim \langle \delta v_0^2 \rangle / v_{e0}^2 < 1$), the critical point, of course, moves inward (from $r_c = 1.75 r_0$) toward the atmospheric base ($r_c = r_0$). The mass flux ($\propto u_0$) is seen (Figure 11b) to increase with increasing temperature in the region of thermal dominance and to increase with increasing wave-amplitude in the region of wave dominance, as one would expect. Figure 11 illustrates the fact that the solar wind is thermally dominated; the wind models for the cool-giants and supergiants we are considering fall in the region of wave-dominance. The division between the thermally driven and wave-driven winds can be represented approximately by the line (in Figure 11b)

$$\left(\frac{v_T}{v_{e0}}\right)^4 \approx \frac{1}{100}\left(\frac{\delta v_0}{v_{e0}}\right), \tag{74}$$

with both wave pressure and thermal pressure playing a significant role in determining the mass flux in a narrow region around this line. As shown in Section 5, even when Alfvén waves are unimportant in determining the mass flux ($\delta v_0 \ll 100 v_T^4/v_{e0}^3$), they may (for a large enough magnetic field) play an important role in determining the asymptotic flow speed, u_∞.

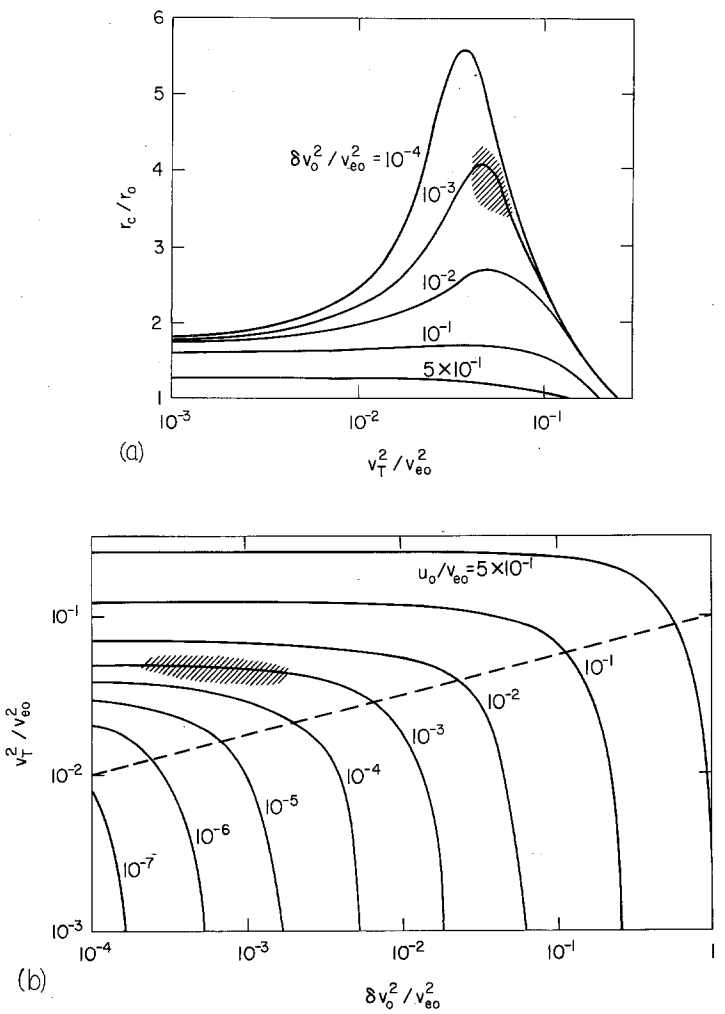

Fig. 11. Alfvén-wave driven stellar winds. (a) Dimensionless critical radius (r_c/r_0) as a function of the dimensionless thermal energy per unit mass (v_T^2/v_{e0}^2) and of the dimensionless wave energy per unit mass ($\langle \delta v_0^2 \rangle / v_{e0}^2$) at the atmospheric base. (b) Dimensionless measure of the stellar mass loss rate (u_0/v_{e0}), as a function of v_T^2/v_{e0}^2 and $\langle \delta v_0^2 \rangle / v_{e0}^2$. The dashed line shows the approximate boundary between thermally dominated mass loss (to the left and above) and wave-dominated mass loss (to the right and below). The hatched areas represent the range of solar wind parameters.

Now let us turn to the subject of the damping of Alfvén waves and its effect on the mass flux and asymptotic flow speed of a wave-driven wind. One can infer from Section 3 that to maintain the large mass flux produced by undamped Alfvén waves (cf. (72)) and to decrease substantially the corresponding asymptotic flow speed (cf. (73)), it is necessary to maintain the work done on the flow by waves in the region of subsonic flow and to minimize the work done in the supersonic region. To do this the waves must be damped just beyond the critical point, and as $r_c \approx 1.75 r_0$ for the wave-driven winds, one would expect the required damping length to be $L \approx r_0$. Hartman and MacGregor (1980) have constructed Alfvén-wave-driven wind models in which the damping length, L, is assumed constant and taken to be $L = R_*$ (where $r_0 = R_*$ and (68) is used). These authors did, indeed, find that this particular damping

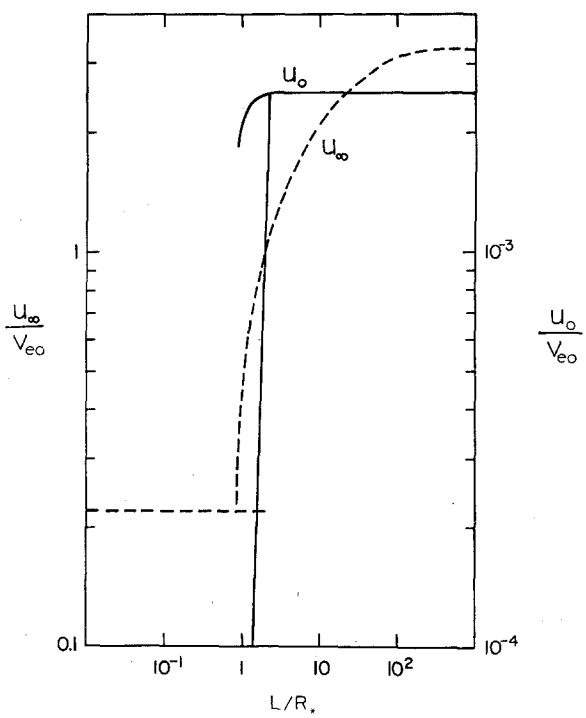

Fig. 12. Asymptotic flow speed in units of gravitational escape speed at the atmospheric base (u_∞/v_{e0}) and a dimensionless measure of the mass loss rate (u_0/v_{e0}) as functions of the Alfvén-wave damping length in units of stellar radii (L/R_*). For strong damping ($L/R_* \ll 1$), the mass loss is negligible and u_∞ corresponds to the solution passing through the outermost (thermal) critical point. For weak damping ($L/R_* \gg 1$), both u_0 and u_∞ correspond to the solution passing through the inner (wave-driven) critical point. For moderate damping ($L/R_* \approx 1$) both critical solutions exist and u_0 and u_∞ for both are shown, the lower values of u_0 and u_∞ corresponding to the solution passing through the outer critical point. Parameters corresponding to model 6 of Hartmann and MacGregor (1980) have been used: $M_* = 16 M_\odot$, $R_* = 400 R_\odot$, $T = 10^4$ K, $n_0 = 10^{11}$ cm^{-3}, $B_0 = 10$ G, $f_{w0} = 3.36 \times 10^6$ erg cm^{-2} s^{-1}, $\mu = 0.667\, m_H$.

length leads to a large mass flux and an asymptotic flow speed less than the surface escape speed. One might ask, however, just how sensitive these results are to the choice of the damping length and what physical mechanism(s) can produce the required damping length. The first of these questions is answered in Figure 12, where the mass flux ($\propto u_0$) and asymptotic flow speed are shown over a range of damping lengths for the stellar parameters used by Hartmann and MacGregor (1980) in their model 6. For $L < 0.85R_*$ the waves are damped so rapidly that they cannot drive a wind, but the thermal pressure gradient in the (assumed) isothermal atmosphere drives a wind that is subsonic out to $r_c = 31.4R_*$ and has a small mass flux and low asymptotic flow speed ($u_\infty = 0.22v_{e0}$). For $0.85R_* < L < 2.25R_*$ both thermally driven ($r_c = 31.4R_*$) and wave-driven ($r_c \approx 1.75R_*$) winds are possible, the former exhibiting a mass flux that increases very rapidly with increasing L and the latter exhibiting a uniformly large mass flux. The thermally driven wind again has a low asymptotic flow speed, but the wave-driven wind has a flow speed that increases rapidly with increasing L, such that $u_\infty > v_{e0}$ for $L > 1.9R_*$. For $L > 2.25R_*$, only a wave-driven wind exists, but its large mass flux is accompanied by a high asymptotic flow speed. Hence, only for a very small range of damping lengths ($0.85R_* < L < 1.9R_*$) can a wind with large mass flux and a relatively low asymptotic flow speed ($u_\infty < v_{e0}$) be produced. The range is much smaller ($0.85R_* < L < 1.0R_*$) if something nearer the inferred observational constraint on flow speed is applied (viz., $u_\infty < v_{e0}/2$). Certainly, the large-mass-flux, low-asymptotic-flow-speed solutions to (69) that Hartmann and MacGregor (1980) showed would not seem to be typical of Alfvén-wave-driven stellar winds.

The question arises as to whether such solutions are at all physically relevant: viz., is there a physical mechanism which might lead to wave damping that would produce the same effect on the wind as a constant damping length of $L \approx R_*$? Hartmann and MacGregor (1980) considered frictional damping (e.g., Osterbrock (1961), Kulsrud and Pierce (1969)), for which $L \propto \omega^{-2}$, and they noted that for their stellar parameters $L = R_*$ would correspond to $\omega = 3.55 \times 10^{-4}\ \mathrm{s}^{-1}$ (i.e., a wave period of nearly 5 hr). Obviously, for any reasonably broad wave spectrum, most of the energy flux carried by Alfvén waves would be damped on a scale outside the range $0.85R_* < L < 1.0R_*$, with the low-frequency waves damped more quickly and the high-frequency waves damped more slowly. (Of course, the frictional damping process depends not only on frequency, but also on density, temperature, ionization fraction, and magnetic field intensity, so L generally varies by several orders of magnitude over a few stellar radii outward from the stellar surface.) Other damping processes, such as those involving nonlinear interactions or mode-conversion, will also lead to an effective damping length of $L \approx R_*$ only for a small range of stellar parameters, if at all (e.g., Holzer *et al.*, 1982).

Although we are forced to conclude that a low asymptotic flow speed ($u_\infty^2 \ll v_{e0}^2$) will probably not be produced in an Alfvén-wave driven stellar wind, we need not necessarily conclude that the massive winds from cool giants and supergiants are not driven by Alfvén waves. This is because in these wave-driven winds the asymptotic flow speed may not be approached until $u \gtrsim v_A$, which may occur farther from the star than the point at which observers normally infer asymptotic flow speed. In other words, stellar

wind observers must make sure they are measuring u_∞ and not the flow speed in, say, the region beyond which little spectral information about the atmosphere is available, because of its low density. In any case, if $u_\infty^2 \ll v_{e0}^2$, then almost any mechanism for driving the stellar wind will face problems similar to those faced by the Alfvén-wave mechanism.

7. Closing Remarks

In this review, we have discussed critically recent research on the acceleration of the solar wind (and of related stellar winds), giving emphasis to high-speed solar wind streams emanating from solar coronal holes. We have seen that existing conductive solar wind models cannot produce high-speed streams with a reasonable mass flux (given a reasonable coronal base pressure), although more realistic descriptions of the thermal conduction could modify this result (Olbert, 1981). It seems, therefore, that the addition of energy to the solar wind above the coronal base is required to accelerate the wind to speeds at 1 AU of more than 600 km s^{-1}. A significant fraction of this energy must be added in the region of supersonic flow in order to increase the flow speed, because subsonic energy addition tends to increase the solar wind mass flux as much as or more than the solar wind energy flux (thus producing little change in or a decrease of the wind energy-per-unit mass, which determines the flow speed at 1 AU).

The energy that must be added to the solar wind to produce high speed streams may be supplied in any number of ways, but we have chosen to concentrate, for illustrative purposes, on Alfvén waves, because they are relatively easy to describe and have been quite well studied. One should not, however, conclude that the Alfvén wave is likely to be the most important type of hydromagnetic wave in accelerating the solar wind or other stellar winds. In a fluctuating, magnetized atmosphere, all hydromagnetic wave modes will be present and will be exchanging energy with each other, and any or all or none may play a significant role in accelerating the wind. For example, it is possible that the refractive properties of fast-mode waves may enable them to drive high-speed solar wind streams in coronal holes, despite a modest upward wave energy flux density at the coronal base (Habbal *et al.*, 1982). In any case, certain aspects of the physical effects involved in the interaction of Alfvén waves with the solar (a stellar) atmosphere and wind are common to other hydromagnetic modes and an understanding of these effects should provide a useful basis for studying the other modes and even other processes not involving hydromagnetic waves.

There have recently been suggestions of alternative mechanisms for the acceleration of the solar wind which we have not touched on in this review. R. N. Thomas and his colleagues (see Heidman and Thomas (1980) and references therein) have suggested that a stellar chromosphere, corona, and wind have a common origin in an intrinsic mass flux from within a star, and that the stellar corona plays no role in the determination of the mass flux, but that the conversion of flow energy to internal energy plays a significant role in heating the chromosphere and corona. This suggestion, which contrasts sharply with Parker's theory (cf. Sections 2 and 3), has not been worked out in detail by Thomas

and colleagues, and the only quantitative analyses of it that have been made have failed to provide any support for it (Parker, 1981; Wolfson and Holzer, 1982). Another suggestion of a solar wind acceleration mechanism involves the revival by Pneuman (1982) of Schlüter's 'melon seed' model for ejecting a bubble of magnetized plasma from the solar atmosphere (Schlüter, 1957; Parker, 1957). The driving force expelling such a bubble is the Lorentz force, and the excess energy necessary for the bubble to escape the solar gravitational field is provided by the injection of the bubble into the atmosphere, which serves to distort (thus adding energy to) the ambient magnetic field. No quantitative analyses have yet been presented to describe the formation and injection of the bubble and to indicate the magnitude of the effect such bubbles might have on the solar wind, so we cannot yet evaluate the possible relevance of such an acceleration mechanism.

Acknowledgements

We are grateful to B.C. Low for his careful reading of and useful comments on the manuscript, to R. G. Athay and A. J. Hundhausen for several valuable discussions, and to A. K. Lynch for typing the manuscript. Two of us (E. L. and T. F.) express our gratitude for the hospitality of R. MacQueen and the High Altitude Observatory during our visit.

References

Alazraki, G. and Couturier, P.: 1971, *Astron. Astrophys.* **13**, 380.
Alfvén, H. and Fälthammar, C.-G.: 1963, *Cosmical Electrodynamics*, Oxford.
Altschuler, M. D., Trotter, D. E., and Orrall, F. Q.: 1972, *Solar Phys.* **26**, 354.
Athay, R. G. and White, O. R.: 1979a, *Astrophys. J. Suppl.* **39**, 333.
Athay, R. G. and White, O. R.: 1979b, *Astrophys. J.* **229**, 1147.
Axford, W. I.: 1968, *Space Sci. Rev.* **8**, 331.
Barnes, A.: 1969, *Astrophys. J.* **155**, 311.
Barnes, A.: 1975, *Rev. Geophys. Space Phys.* **13**, 1049.
Barnes, A.: 1979, in *Solar System Plasma Physics*, Vol. I, North-Holland, Amsterdam.
Beicher, J. W.: 1971, *Astrophys. J.* **168**, 509.
Belcher, J. W. and Davis, Jr., L.: 1971, *J. Geophys. Res.* **76**, 3534.
Belcher, J. W. and Olbert, S.: 1975, *Astrophys. J.* **200**, 369.
Bell, B. and Noci, G.: 1976, *J. Geophys. Res.* **81**, 4508.
Biermann, L.: 1951, *L. Astrophys.* **29**, 274.
Birkeland, K.: 1908, *The Norwegian Aurora Polaris Expedition 1902-1903*, Vol. I, H. Aschehoug and Co., Christiania.
Birkeland, K.: 1913, *The Norwegian Aurora Polaris Expedition 1902-1903*, Vol. II, H. Aschehoug and Co., Christiania.
Bonetti, A., Bridge, H. S., Lazarus, A. J., Lyon, E. J., Rossi, R., and Scherb, F.: 1963, *J. Geophys. Res.* **68**, 1963.
Bretherton, F. P.: 1970, in *Mathematical Problems in the Geophysical Sciences*, American Mathematical Society, Providence.
Cassinelli, J. P.: 1979, *Ann. Rev. Astron. Astrophys.* **17**, 275.
Cassinelli, J. P. and MacGregor, K. B.: 1982, To appear in Sturrock, P. A., Holzer, T. E., Mihalas, D., and Ulrich, R. (eds.), *Physics of the Sun*, The National Academy of Sciences, Washington, D. C.
Chapman, S.: 1957, *Smithsonian Contrib. Astrophys.* **2**, 1.

Chapman, S. and Bartels, J.: 1940, *Geomagnetism*, Clarendon, Oxford.
Chapman, S. and Cowling, T. G.: 1939, *Mathematical Theory of Non-uniform Gases*, Cambridge University Press.
Dewar, R.: 1970, *Phys. Fluids* **13**, 2710.
Durney, B. R.: 1972, *J. Geophys. Res.* **77**, 4042.
Durney, B. R. and Hundhausen, A. J.: 1974, *J. Geophys. Res.* **79**, 3711.
Feldman, W. C., Asbridge, J. R., Bame, S. J. and Gosling, J. T.: 1977, in O. R. White (ed.), *The Solar Output and Its Variation*, Colorado Associated University Press.
Ferraro, V. C. A. and Plumpton, C: 1958, *Astrophys. J.* **127**, 459.
Gingerich, O., Noyes, R. W., Kalkofen, W., and Cuny, Y.: 1971, *Solar Phys.* **18**, 347.
Gringauz, K. T., Bezrukikh, V. V., Ozerov, V. D., and Rybchinskiy, R. E.: 1960, *Soviet Phys. 'Doklady'* (English Transl.) **5**, 361.
Gringauz, K. T., Bezrukikh, V. V., Ozerov, V. D., and Rybchinskiy, R. E.: 1961, *Space Res.* **2**, 539.
Gringauz, K. T., Bezrukikh, V. V., Ozerov, V. D., and Rybchinskiy, R. E.: 1967, *Cosmic Research* **5**, 216.
Habbal, S. R., Flå, T., Holzer, T. E., and Leer, E.: 1982, submitted to *Astrophys. J.*
Habbal, S. R., and Tsinganos, K. C.: 1982, submitted to *J. Geophys. Res.*
Hansen, R. T., Hansen, S. F., and Sawyer, C.: 1976, *Planet. Space Sci.* **24**, 381.
Hartmann, L. and MacGregor, K. B.: 1980, *Astrophys. J.* **242**, 260.
Heidmann, N. and Thomas, R. N.: 1980, *Astron. Astrophys.* **87**, 36.
Heinemann, M. and Olbert, S.: 1980, *J. Geophys. Res.* **85**, 1311.
Hollweg, J. V.: 1972, *Cosmic Electrodyn.* **2**, 423.
Hollweg, J. V.: 1973, *Astrophys. J.* **181**, 547.
Hollweg, J. V.: 1976, *J. Geophys. Res.* **81**, 1649.
Hollweg, J. V.: 1978a, *Rev. Geophys. Space Phys.* **16**, 689.
Hollweg, J. V.: 1978b, *Solar Phys.* **56**, 305.
Hollweg, J. V.: 1982, personal communication.
Holzer, T. E.: 1979, in *Solar System Plasma Physics*, Vol. I, North-Holland, Amsterdam.
Holzer, T. E. and Axford, W. I.: 1970, *Ann. Rev. Astron. Astrophys.* **8**, 30.
Holzer, T. E., Flå, T., and Leer, E.: 1982, To be submitted to *Astrophys. J.*
Holzer, T. E. and Leer, E.: 1980, *J. Geophys. Res.* **85**, 4665.
Hundhausen, A. J.: 1972, *Coronal Expansion and Solar Wind*, Springer, New York.
Hundhausen, A. J.: 1977, in J. B. Zirker (ed.), *Coronal Holes and High Speed Wind Streams*, Colorado Associated University Press.
Hundhausen, A. J., Hansen, R. T., Hansen, S. F., Feldman, W. C., Asbridge, J. R., and Bame, S. J.: 1976, in *Physics of Solar Planetary Environments*, American Geophysical Union, Washington, D. C.
Hundhausen, A. J. and Holzer, T. E.: 1980, *Phil. Trans. Roy. Soc. London* **A297**, 521.
Jacques, S. A.: 1977, *Astrophys. J.* **215**, 942.
Kopp, R. A. and Holzer, T. E.: 1976, *Solar Phys.* **49**, 43.
Krieger, A. S., Timothy, A. F., and Roelof, E. C.: 1973, *Solar Phys.* **29**, 505.
Kulsrud, R. and Pierce, W. P.: 1969, *Astrophys. J.* **156**, 445.
Leer, E., Flå, T., and Holzer, T. E.: 1980, *Il Nuovo Cimento* **36**, 114.
Leer, E. and Holzer, T. E.: 1979, *Solar Phys.* **63**, 143.
Leer, E. and Holzer, T. E.: 1980, *J. Geophys. Res.* **85**, 4681.
Munro, R. H. and Jackson, B. V.: 1977, *Astrophys. J.* **213**, 874.
Neupert, W. M. and Pizzo, V. A.: 1974, *J. Geophys. Res.* **79**, 3701.
Neugebauer, M. and Snyder, C. W.: 1966, *J. Geophys. Res.* **71**, 4469.
Nolte, J. T., Krieger, A. S., Timothy, A. F., Gold, R. E., Roelof, E. C., Vaiana, G., Lazarus, A. J., and Sullivan, J. D.: 1976, *Solar Phys.* **46**, 303.
Olbert, S.: 1981, in *Proceedings of an International School and Workshop on Plasma Astrophysics* ESA SP-161.
Osterbrock, D. E.: 1961, *Astrophys. J.* **134**, 347.
Parker, E. N.: 1957, *Astrophys. J. Suppl.* **3**, 51.
Parker, E. N.: 1958, *Astrophys. J.* **128**, 664.
Parker, E. N.: 1960, *Astrophys. J.* **132**, 821.
Parker, E. N.: 1963, *Interplanetary Dynamical Processes*, Interscience, New York.
Parker, E. N.: 1964a, *Astrophys. J.* **139**, 72.
Parker, E. N.: 1964b, *Astrophys. J.* **139**, 93.

Parker, E. N.: 1965, *Space Sci. Rev.* **4**, 666.
Parker, E. N.: 1981, *Astrophys. J.* **251**, 266.
Perkins, F.: 1973, *Astrophys. J.* **179**, 637.
Pneuman, G. W.: 1980, *Astron. Astrophys.* **81**, 161.
Pneuman, G. W.: 1982, submitted to *Astrophys. J.*
Scherb, F.: 1964, *Space Res.* **4**, 797.
Schlüter, A.: 1957, in H. C. van de Hulst (ed.), *Radio Astronomy, IAU Symp.* **4**, 356.
Scudder, J. D. and Olbert, S.: 1979a, *J. Geophys. Res.* **84**, 2755.
Scudder, J. D. and Olbert, S.: 1979b, *J. Geophys. Res.* **84**, 6603.
Sheeley, Jr., N. R., Harvey, J. W., and Feldman, W. C.: 1976, *Solar Phys.* **49**, 271.
Snyder, C. W. and Neugebauer, M.: 1964, *Space Res.* **4**, 89.
Spitzer Jr., L.: 1962, *Physics of Fully Ionized Gases*, Interscience, New York.
Vernazza, J. E., Avrett, E. H., and Loeser, R.: 1973, *Astrophys. J.* **184**, 605.
Wagner, W. J.: 1976, *Astrophys. J.* **206**, 583.
Weber, E. J. and Davis Jr., L.: 1967, *Astrophys. J.* **148**, 217.
Withbroe, G. L.: 1977, in *Proceedings of the November 7–10, 1977 OSO-8 Workshop*, LASP, University of Colorado.
Withbroe, G. L.: 1982, *Space Sci. Rev.*
Wolfson, R. L. T. and Holzer, T. E.: 1982, *Astrophys. J.* **255**, 610.